FABRICATION OF A BIONANOCOMPOSITE SCAFFOLD BY CROSSLINKING AMINE-FUNCTIONALIZED GOLD NANOPARTICLES WITH PORCINE CHOLECYSTIC EXTRACELLULAR MATRIX

DISSERTATION BY

JIMNA MOHAMED AMEER

REG.NO: 07/M.Phil/2015

IN PARTIAL FULFILLMENT OF THE REQUIREMENTS FOR THE DEGREE OF

MASTER OF PHILOSOPHY IN BIOMEDICAL TECHNOLOGY

BIOMEDICAL TECHNOLOGY WING

SREE CHITRA TIRUNAL INSTITUTE FOR MEDICAL SCIENCES AND TECHNOLOGY ,THIRUVANANTHAPURAM- 695012

2016

DECLARATION

I hereby declare that the dissertation entitled "**Fabrication of a bionanocomposite scaffold by crosslinking amine-functionalized gold nanoparticles with porcine cholecystic extracellular matrix**" submitted to Sree Chitra Tirunal Institute for Medical Sciences and Technology(SCTIMST), Thiruvananthapuram, in partial fulfillment for the degree of Master of Philosophy in Biomedical Technology is a record of original work carried out by me under the guidance of Dr. T.V. Anilkumar, Scientist F, in the Division of Experimental Pathology, Biomedical Technology Wing, SCTIMST, Kerala, during the period of January 2016 to June 2016.

I further declare that the results of the work have not been previously submitted for any other degree or fellowships.

Place: Thiruvananthapuram

Date: 30.06.2016

Jimna Mohamed Ameer

Reg. No: 2015/Mphil/07

Roll No: 160020

BIOMEDICAL TECHNOLOGY WING

SREE CHITRA TIRUNAL INSTITUTE FOR MEDICAL SCIENCES & TECHNOLOGY

THIRUVANANTHAPURAM-695012, INDIA

(An Institute of National Importance under Govt. of India)

CERTIFICATE

This is to certify that Ms. Jimna Mohamed Ameer from the Division of Experimental Pathology of this institute has fulfilled the requirements prescribed for the M. Phil. degree of the Sree Chitra Tirunal Institute for Medical Sciences and Technology, Thiruvananthapuram. The dissertation entitled, "**Fabrication of a bionanocomposite scaffold by crosslinking amine-functionalized gold nanoparticles with porcine cholecystic extracellular matrix**" was carried out under my supervision. No part of the thesis was submitted for the award of any degree or diploma prior to this date.

Place: Thiruvananthapuram

Date: 30.06.2016

Dr. T.V. Anilkumar

Scientist F

Division of Experimental

Pathology

The dissertation entitled

“FABRICATION OF A BIONANOCOMPOSITE SCAFFOLD BY CROSSLINKING AMINE-FUNCTIONALIZED GOLD NANOPARTICLES WITH PORCINE CHOLECYSTIC EXTRACELLULAR MATRIX”

Submitted by

Jimna Mohamed Ameer

for the degree of

Master of Philosophy in Biomedical Technology

BIOMEDICAL TECHNOLOGY WING

SREE CHITRA TIRUNAL INSTITUTE FOR MEDICAL SCIENCES AND TECHNOLOGY, THIRUVANANTHAPURAM- 695012

is evaluated and approved by

.....	…….....
Dr.T.V.Anilkumar,	Examiner
Scientist F (Research Supervisor)	
Division of Experimental Pathology	

ACKNOWLEDGEMENTS

I am deeply indebted to my supervising guide Dr. T. V. Anilkumar, Scientist F, Experimental Pathology Division, SCTIMST for his guidance and support for the completion of my work. It was a very enriching experience for me all along six months of dissertation work. He allowed me to work with complete intellectual freedom. The encouragement, the inspiration received all through these days will always help me in future. I would like to express my hearty thanks to my co-guide Ms. Reshma S, PhD scholar, Division of Experimental Pathology, SCTIMST for the timely criticism of work and fruitful discussions. I would like to express a special note of gratitude for her help, suggestions and constant support throughout the study. I am thankful to all the staffs of Experimental Pathology for their support and encouragement. Special thanks to my lab members, Dr. Geetha. C.S (Junior Scientific Officer), Dr. Akhila Rajan (Research Associate), Ms. Manjula. P. M. (PhD student), Ms. Reshmi Raj (PhD student), my seniors Dr. Deepa. R and Dr. Jaseer Muhammed C.J for their valuable support throughout my work.

I express my respect and gratitude to Dr. Rekha. M. R (Biosurface Technology) and Dr. Kalyana Krishnan (Division of Dental products) for giving me consent to use particle size analysis equipment and Ms. Vibha for helping me in particle size analysis. I am also indebted to Dr Prabha D Nair for her timely help in allowing me to use their lab equipments which lead to the successful completion of my project.

I gratefully acknowledge Mr. Nishaad (Technical assistant) for his help in Environmental Scanning Electron Microscopy and Mr Francis and Ms. Susan for their help in Transmission Electron Microscopy. I would like to thank Mr. Vineeth (PhD student), Mr. Ansar EB(Research Associate) and Ms. Shanthi (PhD student) for their help and valuable suggestions in FTIR analysis..

I am extremely thankful to my batch mates who were with me all the time, understanding, and supporting me whenever I feel discouraged and dejected.

I express my deep sense of gratitude to Dr. Manoj Komath and Dr Maya, M.Phil Coordinators and Dr. Jayabalan Muthu, Former M.Phil Coordinator SCTIMST for their academic assistance.

Without the prayer, support, patience, encouragement, love and care from my family, especially my father Mr. S.M Ameer, I could not have finished my study.

Finally, I humbly bow before the almighty for giving me the strength, wisdom and luck to complete this dissertation.

Jimna Mohamed Ameer

ABBREVIATIONS

µg	-	Microgram
˚C	-	Degree Celsius
AuNp	-	Gold Nanoparticles
C-ECM	-	Cholecystic Extracellular Matrix
Cys-AuNp	-	Cysteine Capped Gold Nanoparticles
Cys-AuNp CECM	-	Cys AuNp Modified CECM
DLS	-	Dynamic Light Scattering
DMSO	-	Dimethyl Sulfoxide
DMEM	-	Dulbecco's Minimum Essential Medium
ECM	-	Extracellular Matrix
ESEM	-	Environmental Scanning Electron Microscopy
FDA	-	Fluorescein diacetate
FBS	-	Foetal Bovine Serum
FTIR	-	Fourier Transform Infrared Spectroscopy
IR	-	Infrared
GSH	-	Glutathione Reduced
GSH-AuNp CECM	-	GSH AuNp Modified CECM
H9c2	-	Cardiomyoblast cell line

MMP	-	Matrix Metalloproteinase
MSC	-	Mesenchymal stem cells
MTT	-	Methyl thiazolyl tetrazolium
nm	-	Nanometer
NaCl	-	Sodium Chloride
OD	-	Optical Density
PDI	-	Polydispersity Index
PI	-	Propidium Iodide
SD	-	Standard Deviation
SIS	-	Small Intestinal Submucosa

LIST OF FIGURES

CONTENTS

ABSTRACT

Extracellular matrix isolated from organs and tissues of animals are excellent sources of scaffold useful for tissue engineering and regenerative medicine applications. Porcine cholecystic extracellular matrix (C-ECM) has been found to be a biomaterial, rich in structural and functional proteins. This study aimed to fabricate a bionanocomposite scaffold by conjugating amine-functionalized gold nanoparticles on porcine cholecystic extracellular matrix. Gold nanoparticles were synthesized by conventional citrate reduction method and then functionalized by cysteine or glutathione. These were characterized by UV-visible Spectrophotometry, Transmission Electron Microscopy and Dynamic Light Scattering. The amine-functionalized gold nanoparticles were then conjugated on to C-ECM scaffold by EDC/NHS chemistry-based crosslinking. Incorporation of gold nanoparticle onto the scaffold was confirmed by Energy Dispersive Spectroscopy and Thermogravimetric Analysis. Subsequently the biomaterial properties of the bionanocomposites were evaluated as a scaffold for potential cardiac tissue engineering application. Conjugation of the amine-functionalized gold nanoparticle onto the scaffold increased the conductivity of the cholecystic extracellular matrix. The bionanocomposite prepared by conjugating cysteine functionalized gold nanoparticles had biomaterial properties of candidate scaffolds desired for cardiac tissue engineering application.

INTRODUCTION

Tissue engineering scaffolds of mammalian origin have been used for treating a variety of diseases. They are essentially, extracellular matrices of organs/tissues of heterogenic or xenogenic origin (Badylak, 2004). The biomaterial quality of these scaffolds depends on the donor species, source organ/tissue, the technique used for preparation of the scaffold and the modality for terminal sterilization/storage. Although porcine small intestinal submucosa (SIS) is the most favourite source of extracellular matrix in this category, commercial products prepared from other organs/tissues have also been used for fabricating bioartificial organs. For example, human-derived allograft (GraftJacket®), Silicone membrane/reconstituted bovine collagen matrix (INTEGRA™ Bilayer Matrix), Equine pericardium xenograft (Unite®) have found excellent clinical uses. Indeed, one of the prominent uses of SIS is cardiac tissue engineering, CorMatrix® fabricated out of SIS facilitates tissue regeneration and regrowth, when used as xenograft for repairing cardiac and vascular (Nezhad et al., 2016). Gold-impregnated scaffolds showed a stronger contraction force, faster calcium transients, and a lower excitation threshold. These are all effects that are seemingly related to the electrical conductivity of the non-immunogenic gold nanoparticles (Shevach et al., 2014).

The host laboratory has an interest in using porcine cholecyst-derived extracellular matrix (C-ECM) for biomedical applications. C-ECM is an acellular natural biodegradable matrix having mesh like architecture (Burugapalli et al., 2007) with macromolecules and mechanical properties (Coburn et al., 2007) suitable for tissue engineering. It supports proliferation of valvular endothelial cells *in vitro* (Brody et al., 2007). Further, the extent of cross linking and functionalization of the matrix can be modulated (Burugapalli et al., 2014, 2009; Chan et al., 2008) as required for specific tissue engineering application. Moreover, observations through animal

experiments have indicated that, it is a candidate biomaterial for fabricating buttressing staples for gastrointestinal resection (Burugapalli et al., 2008) and skin wound healing matrix (Revi et al., 2013). A non-detergent/enzymatic method (Anilkumar et al., 2014) for preparing C-ECM scaffold which has low immunogenicity (Muhamed et al., 2015a, Muhamed etal., 2015b) that promotes faster healing of skin excision (Revi et al., 2013) and burn wounds (Revi et al., 2016). Probably, the C-ECM has other utilities as well similar to those prepared from SIS that are already in market.

Ideal cardiac tissue construct should provide optimal structural, mechanical and electrophysiological properties (Wang et al., 2010). Relevant modifications on C-ECM can improve its properties as a potential bioscaffold for cardiac tissue engineering. Gold nanoparticles can be incorporated into the C-ECM thereby improving its conductive property.

Hypothesis

This study is centered on the hypothesis that conjugation of amine functionalized gold nanoparticle modulates the quality of porcine cholecystic extracellular matrix as a scaffold for cardiac tissue engineering.

Objectives

In consistence with the above hypothesis, the study aimed to fabricate a bionanocomposite scaffold by conjugating amine functionalized gold nanoparticle on porcine cholecystic extracellular matrix and evaluated its biomaterial properties as a scaffold for cardiac tissue engineering. The specific objectives were the following:

- Synthesis of gold nanoparticle by citrate reduction method.
- Amine functionalization of the gold nanoparticles by two methods: with L-Cysteine and L-Glutathione.

- Preparation of Cholecystic Extracellular matrix (C-ECM).
- Coupling of gold nanoparticles to C-ECM by two methods: Direct infiltration and Chemical crosslinking.
- Chemical and biological evaluation of the above four scaffolds.

REVIEW OF LITERATURE

Diseases, injury and trauma can lead to damage and degeneration of tissues in human body and transplantation is a treatment strategy (Langer, 2000). The treatment mainly focused on transplantation of tissues from one site to another in the same patient (autograft) or from one individual to another (transplant or allograft). But many difficulties were found in using these methods of treatment. Harvesting autografts resulted in new injury at the donor-site and this treatment strategy was painful and expensive. Similarly allograft transplantation also caused serious constraints due to problems like availability of enough tissue for the patients, also risks of rejection by the patient's immune system and possibility of infection and diseases from the donor. The field of tissue engineering aims to regenerate the damaged tissues by the development of biological substitutes that helped in repair, regeneration and thereby maintaining the tissue function (Langer, 2000). Scaffolds plays an important role in remodelling of tissues. Numerous scaffolds for tissue regeneration are developed from a large variety of materials like polymer, ceramics, metal particles etc by using different fabrication techniques such as electrospinning, freeze drying etc (Lu et al., 2013). Regardless of the tissue type, a number of key considerations are important when designing or determining the suitability of scaffold for tissue regeneration (O'Brien, 2011). The first criteria for any scaffold for tissue regeneration is that it should be biocompatible and after implantation it must produce negligible immune reaction. Biodegradability of a scaffold is also important as the objective of tissue engineering is the replacement of the substitute by body's own cells (O'Brien, 2011). Byproducts formed, if any as the result of degradation should also be non-toxic (Babensee et al., 1998). Scaffolds should have desired mechanical properties and porous architecture to ensure cellular penetration and adequate nutrients to the cells within them with respect to their applications (Hutmacher, 2000).

Extracellular Matrix

Extracellular matrix (ECM), a composite of structural and functional proteins, glycoproteins, and glycosaminoglycans arranged in an ultrastructure unique to each tissue and organ, are secreted by the resident cells and exist in a state of reciprocity (Badylak, 2002). ECM provides mechanical support for attached cells, generate signals to maintain cell survival, serve as a substratum for cell migration and proliferation and act as a barrier for the passage of macromolecules. ECM has an important role in transmitting environmental signals to cells which influences the cell proliferation, differentiation and death. Collagen, fibronectin, laminin, elastin and other components like matrix metalloproteinase, bioactive cryptic peptides and growth factors are the major components of ECM (Kular et al., 2014). These proteins perform diverse functions which includes the provision of structural support and tensile strength, attachment sites for cell surface receptors, and also acts as a reservoir for signaling factors that modulates diverse host processes such as angiogenesis, vasculogenesis, cell migration, cell proliferation, inflammation, and wound healing (Badylak, 2007). A diverse array of biologic activities including angiogenesis, anti- angiogenesis, chemotactic effects and anti-microbial effects has been studied for collagen and fibronectin (Houghton et al., 2006; O'Reilly et al., 1997; Ramchandran et al., 1999). Studies showed that the matrix promoted embryonic development and enhanced the fate of stem cell differentiation (Murry and Keller, 2008). Research on ECM started since decades and the current understanding of ECM is that it influences cellular activity and responses. There were two areas of great interest, (1)the influence of ECM at biomechanical and molecular level and it impact on cell differentiation profile (Engler et al., 2006) and (2) to understand the role of ECM in anchoring cells (Larsen et al., 2006). The actual composition and ultrastructure of the ECM is only partially identified. Therefore, it is difficult to design and

engineer a mimic of the complex structure of ECM. Decellularization was identified as an effective method for harvesting extracellular matrix from parent tissues. Many biomedical device products composed of xenogeneic and allogenic extracellular matrix exist currently but their performance depends upon the source of origin, methods of preparation and applications. ECM acts as an ideal biological scaffold for tissue regeneration as it supported the reconstruction of damaged or missing tissues. ECM has been isolated from different mammalian tissues and organs including liver, urinary bladder, arterial vasculature, heart valve dermis and small intestine (Armour et al., 2006; Badylak et al., 1989; Brown et al., 2006; Cebotari et al., 2006; Chen et al., 1999; Walles et al., 2003).

Composition of Extracellular Matrix

ECM comprises multiple matrix proteins, and these proteins provided the necessary support to cells and tissues (Eckes et al., 2010). Depending on their function, they were categorized as structural and non-structural proteins. Examples of structural proteins are collagens and elastins with fibronectin, laminin and tenascin as non-structural proteins. Integrins, growth factors and group of matrix metalloproteineases (Brown and Badylak, 2014) also comprise the ECM. These proteins are secreted into the extracellular space where they are capable of self-assembling into an interconnected three-dimensional network, as depicted in Fig.1

Collagen is the most abundant protein within the body and is found amassed in the ECM of the connective tissues such as tendon and skin. The predominant form of structural proteins provides tensile strength, cell adhesion and cell migration. More than 30 types of collagen have been identified although not all of them are found in ECM (Heino, 2007).

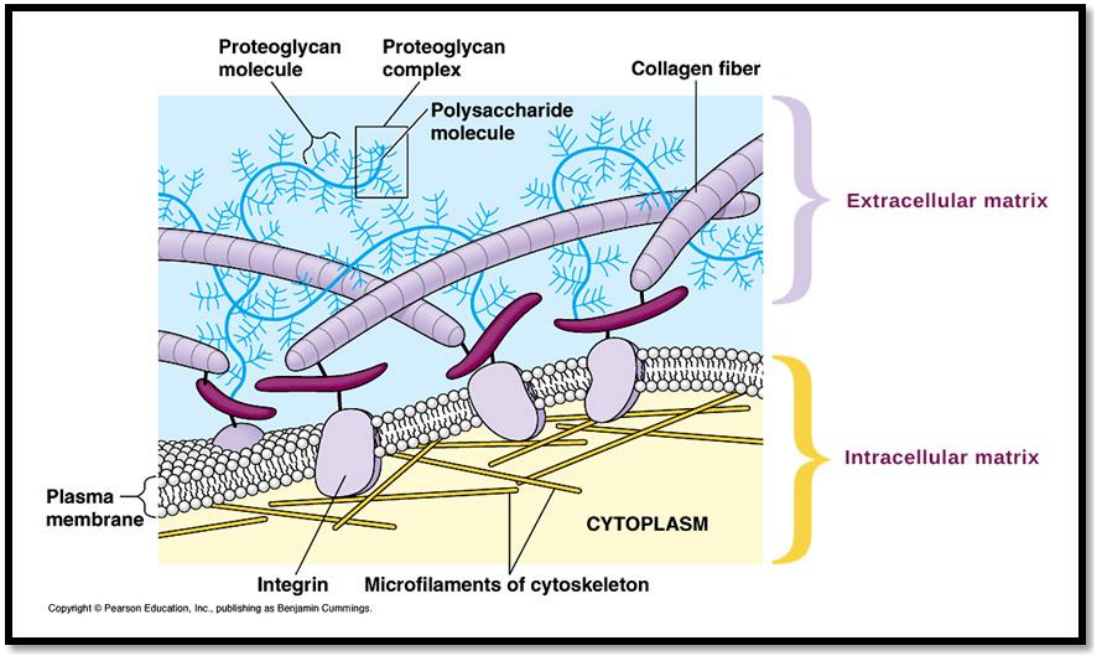

Fig 1. Overview of macromolecular structure of extracellular matrix

The fibril arrangement of collagen provided tensile strength to tissues and allowed them to withstand different mechanical stress. Decorin and fibromodulin regulate collagen fibril formation in the ECM. Collagen type I is predominant in all tissues, and abundantly found in tendons and skin. Collagen type II is found in cartilage and cornea whereas collagen III is the major form within the blood vessel walls. Fibroblasts and endothelial cells synthesize collagen (Bosman and Stamenkovic, 2003). Elastin is another structural protein which predominates and found closely linked to collagen. It provided the ability to enhance the continuous stretching of the tissue in dermis of skin (Kular et al., 2014). Fibronectin is located within the basement membrane and plays a key role in both cell adhesion and wound healing response to injury. Fibronectin is arranged as mesh of fibrils same as that of collagen and found as crosslinked to integrins like cell surface receptors (Tanzer, 2006).

Laminins are glycoproteins with trimeric structure that are involved in cell adhesion, differentiation and migration. Studies showed that the first proteins of ECM found in embryos

was laminins and it played an important role in differentiation of cells in nerves and blood vessels (Domogatskaya et al., 2012). Tenascins are group of ECM proteins that have been linked to the mechanical activity. Vascular endothelial growth factor (VEGF), fibroblast growth factor (FGF) and transforming growth factor β (TGF-β) were examples of growth factors that was tied to the ECM through either heparan or heparan sulphate (Hynes, 2009). Matrix metalloproteinases (MMPs) are enzymes involved in the disintegration of the ECM. The breakdown of the matrix formed a part of the on-going remodeling of ECM. This transformation process was found to be critical during neovascularization and bone remodeling (Streuli, 1999).

Role of ECM in Tissue Engineering

The ECM plays an important role in differentiation of stem cells. It has been studied that ECM from young mesenchymal stem cells (MSCs) displayed significantly higher levels of protein expression (Choi et al., 2011). Studies on ECM also revealed its significant role in cell adhesion, migration and proliferation. It can also manipulate the differentiation of MSCs through its stiffness with stem cells by changing their properties by the underlying substrata. This highlighted the critical nature of the mechanical signals that are passed on to cells from the ECM, and the importance of the relationship between cells and their environment in determining the commitment to a certain cell lineage (Kular et al., 2014). The ECM, typically from xenogeneic sources has been used for the replacement or regeneration of various tissues. ECM based scaffolds promoted constructive remodeling (Fig.2) depending upon the methods used for scaffold preparation. Different studies have utilized ECM that was derived from organs such as small intestine, cholecyst, omentum, urinary bladder and many other organs also (Burugapalli et al., 2008; Shevach et al., 2014; Shi and Ronfard, 2013). The choice of organs or tissues for ECM isolation depends on the age and physiologic requirements of the particular tissue. An allogeneic

or xenogeneic source of ECM has usually been used, thus providing the possibility of an off-the-shelf product for clinical application. There were differing opinions as to whether the ECM should be seeded with site-specific cells prior to utilization as a repair scaffold or should be used in an acellular form. The effect of seeding cells to an ECM scaffold upon the biologic remodeling response varied depending upon the intended application and the manner of preparation of the composite scaffold. A cellular component requires an autologous cell source and a controlled environment to assure cell viability during the translocation of the cell-scaffold composite to the recipient tissue site. Both cellular and acellular forms of ECM scaffolds have been used for cardiac, skin, vascular and dental tissue engineering applications (Badylak, 2004).

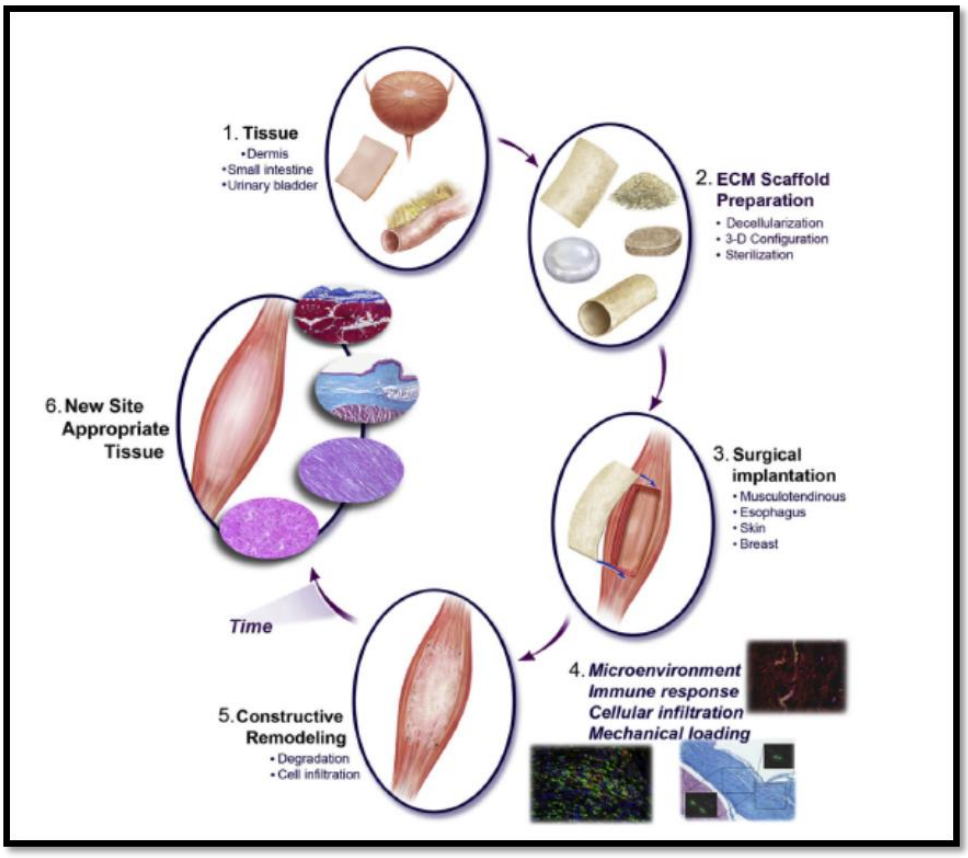

doi:10.1016/j.trsl.2013.11.003

Fig 2. Overview of the constructive remodeling process associated with extracellular matrix (ECM) scaffold implantation.

Decellularization and Fabrication Methods of ECM Scaffolds

The ECM was identified as a highly complex, tissue-specific reservoir of structural and functional proteins, which is capable both of being remodeled by resident cells and of directing cellular behavior, phenotype, and survival. ECM has an important role in development and in the maintenance of stem cell phenotype, and these processes are exquisitely regulated, potentially involving multiple ECM components. Therefore, it was highly desirable to maintain the components of ECM to the highest degree possible. The methods of ECM isolation from source tissue and its manufacture as a scaffold for tissue reconstruction applications must be specifically and carefully tailored to the tissue of interest (Brown and Badylak, 2014; Gilbert et al., 2006). The use of ECM derived from decellularized tissue is increasing in regenerative medicine and tissue engineering strategies. Studies have showed that ECM influence cell mitogenesis, chemotaxis, cell differentiation and induce constructive host tissue remodeling responses by their 3D ultrastructure, composition and surface topology. Therefore tissue processing methods including decellularization determines the quality of ECM and its clinical success (Cebotari et al., 2006; Crapo et al., 2011).The most effective agents for decellularization of each tissue and organ depended upon many factors, including the tissue's cellularity (e.g. liver vs. tendon), density (e.g. dermis vs. adipose tissue), lipid content (e.g. brain vs. urinary bladder), and thickness (e.g. dermis vs. pericardium). It should be understood that every cell removal agent and method altered ECM composition and resulted in some degree of ultrastructure disruption. Minimization of these undesirable effects rather than complete avoidance is the objective of decellularization (Crapo et al., 2011).

Chemical decellularization was performed for the effective removal of antigenic epitopes associated with cell membranes and intracellular components of tissues and organs that was

necessary to minimize or avoid adverse immune response by allogeneic and xenogeneic recipients of ECM scaffold material. Chemical decellularization is usually carried out with enzymes and detergents and the procedure may have deleterious effects on the biomaterial quality of the scaffold. Using chemical agents like acids and bases catalyzed the hydrolytic degradation of biomolecules. Peracetic acid is a common disinfection agent as well as a decellularization agent by removing residual nucleic acids with minimal effect on the ECM composition and structure. Bases (e.g. calcium hydroxide, sodium sulphide, and sodium hydroxide) are harsh enough and commonly used to remove hair from dermis samples during the early stages of decellularization. However, bases completely eliminated growth factors from the matrix and decreased ECM mechanical properties more significantly than chemical and enzymatic agents (Reing et al., 2010). The primary mechanism by which bases such as sodium hydroxide reduced mechanical properties by the cleavage of collagen fibrils and disruption of collagen crosslinks (Crapo et al., 2011; Gorschewsky et al., 2005). Hypertonic saline helped in dissociation of DNA from proteins. Hypotonic solutions readily caused cell lysis by simple osmotic effects with minimal changes in matrix molecules and architecture. Ionic, non-ionic, and zwitterionic detergents solubilized cell membranes and dissociated DNA from proteins, and they were therefore effective in removal of cellular material from tissue. However, these agents also disrupted and dissociated proteins in the ECM as evidenced by their use in protein extraction procedures in tissue proteomics. Physical methods of decellularization involved freeze thawing and by mechanical abrasion in combination with enzymes, hypertonic saline, or chelating agents, all of which facilitated dissociation of cells from their subjacent basement membrane. However, underlying ultrastructure and basement membrane integrity invariably damaged by any direct application of mechanical force (Crapo et al., 2011). Some detergents used to facilitate

decellularization have been shown to disrupt collagen of certain tissues, thereby decreasing the mechanical strength of the tissue, while the same detergent had no effect on the collagen in another tissue. Thus, the decellularization method required optimization for each tissue to remove cellular material without compromising the mechanical properties of the tissue. The potential beneficial effects of biologic scaffolds in the field of tissue engineering and regenerative medicine can be realized if optimal methods of decellularization are employed (Woods and Gratzer, 2005).

Small Intestinal Submucosa Derived Extracellular matrix

Small intestinal submucosa is acellular biological extracellular matrix comprised of collagen, elastin, glycosaminoglycans, proteoglycans and growth factors that significantly improved wound healing. Numerous cell types has found to be attached, proliferated, differentiated and migrated in SIS (Shi and Ronfard, 2013). When wounds are treated with SIS, activity of matrix metalloproteinase decreased. Compared to standard care, SIS significantly promoted wound healing rates (Mostow et al., 2005).Multiple layers of SIS has been tried to improve the mechanical properties of the matrix and it slowly degraded. There are different porcine small intestinal submucosa based products for different applications, Cuffpatch^{TM} , Surgisis® is used soft tissue repair and Durasis® for dura mater repair (Badylak and Gilbert, 2008). A lyophilized sheet form of porcine small intestinal submucosa available as Oasis® promoted partial and full thickness wounds. The SIS wound matrix has been found as an adjunct therapy that significantly improved healing of chronic leg ulcers over compression therapy alone (Mostow et al., 2005) (Nezhad et al., 2016).

Extracellular matrix from xenogeneic origin suffered from large spectrum of heterogeneity in microstructure resulting in inconsistent results. The microarchitecture of small intestinal

submucosa derived scaffold was altered to provide more uniform SIS for better tissue repair and regeneration using nanotechnology. SIS modified with Biodegradable poly(lactic-*co*-glycolic) acid (PLGA) nanoparticles showed enhanced mechanical properties as well as quality of the scaffold (Mondalek et al., 2008). Hyaluronic acid incorporated to SIS through PLGA nanoparticle improved the consistency of the naturally derived biomaterial and bladder regeneration was enhanced in Beagle dogs. The modified grafts showed evidence of improved smooth muscle regeneration on histological assessment (Roth et al., 2011). HA-PLGA modified SIS enhanced angiogenesis and neovascularization in canine bladder augmentation model (Mondalek et al., 2010). Gold nanoparticles are known to be biocompatible and can be easily functionalized with biomolecules like growth factors, DNA, peptides .They are also used as drug delivery system or to target specific cells (Everts et al., 2006). The size and shape of the gold nanoparticles can be adjusted and extensively studied as new contrast agents for imaging and novel photothermal therapies (Chithrani et al., 2006). Gold nanoparticle modified collagen scaffolds showed improved characteristics compared to bare collagen scaffold and have potential as a medium for drug delivery (Castaneda et al., 2008). Cross-linking of 1% collagen gels with gold nanoparticles protected with tiopronin (a multivalent cross-linker) resulted in the formation of an unusual gel morphology: a particulate phase containing interconnected, small collagen-TPAu particles. The gels do not contain visible fibrillar structures, but exhibit larger mechanical stability than non-cross-linked collagen (Schuetz et al., 2013). Polycaprolactone-gelatin scaffold modified with gold nanoparticle enhanced the differentiation, growth and maturation of neurons (Baranes et al., 2016). Decellularised matrices obtained from omentum have been decorated with gold nanoparticle and used for cardiac tissue engineering applications. Gold nanoparticles could significantly increase the conductivity of the natural

material without affecting the mechanical properties relevant for cardiac tissue engineering. Cardiac cells grown on the scaffold exhibited elongated and aligned morphology, massive striation, and organized connexin 43 electrical coupling proteins. Finally, growing cardiac cells in AuNp scaffolds has led to the formation of cardiac patches generating stronger contraction forces (Shevach et al., 2014). CorMatrix® porcine SIS-ECM (CorMatrix Cardiovascular, Inc., Roswell, GA, USA) has also gained popularity in cardiovascular tissue engineering due to its ease of use, remodelling properties, lack of immunogenicity, absorbability and potential to promote native tissue growth (Nezhad et al., 2016).

Cholecystic Extracellular Matrix

One of the popular and favorite scaffold commercially available is small intestinal submucosa derived scaffold (SIS) that helped in constructive remodeling of injured sites in many parts of the body, including chronic wounds such as non-healing leg ulcers. However, some studies also reported that the SIS have no significant beneficial effect in treating full thickness skin wounds in dogs but may elicit some adverse inflammatory response. There are also reports of complications arising from the clinical use of small intestine submucosa in other regenerative medical applications (Zheng et al., 2005). Hence, there is a quest for better biological scaffolds for regenerative medical applications in general and skin graft substitutes in particular. Cholecyst derived extracellular matrix (CEM) recovered from ECM of porcine gallbladder had variable application in the field of regenerative medicine (Shakya et al., 2016). Krishna Burugapally and his co workers in 2007 first reported the evidence of an intact ECM with a mesh like architecture, derived from sub serosal connective tissue of cholecyst (Burugapalli et al., 2007). This work laid the foundation stone for the current development and ongoing researches in C-ECM. The subserosal layer was isolated by mechanical delamination and followed by decellularization with

a treatment with peracetic acid and ethanol solution in water to obtain the final matrix. This study assessed the qualitative and quantitative macromolecular compositions of the matrix and revealed that collagen is the primary structural component of the matrix. It is this collagen fiber architecture which played a critical role in determining biomechanical behavior of the matrix scaffold. In addition to collagen, elastin components are also present. The studies proved that C-ECM is an ideal supporting structure for the attachment and proliferation of murine fibroblasts (Burugapalli et al., 2007). Studies also showed that C-ECM has the ability to support cell growth of different cells and also promote differentiation of cells by providing appropriate stimulus (Burugapalli et al., 2007). Porcine cholecyst derived ECM also acted as buttressing staples for gastro intestinal resection and anastomotic procedures (Burugapalli et al., 2008). C-ECM also supported the proliferation of valvular endothelial cells as well as interstitial cells and acted as an potential substitute for tissue engineered heart valve scaffold (Brody et al., 2007). This matrix was highly rich in collagen and several other macromolecules like elastin, laminin, proteoglycans and other components like growth factors. C-ECM was found to be weakly anisotropic and has the ability to support large strains across a physiological regime (Coburn et al., 2007). Quality of a biomaterial was determined by its chemical content and biomolecular content. C-ECM has identified as a reliable collagen rich natural scaffold for bladder augmentation (Kajbafzadeh et al., 2014). It has also shown to act as an as reinforcing buttressing staples for gastrointestinal resection and anastomotic procedures (Burugapalli et al., 2008).It possessed a micro-architecture similar to heart valves, supported proliferation of valvular endothelial and interstitial cells and also it is proved as a potential skin graft for treating full thickness skin wounds. It also elicited a very less immunogenic potential when compared to other commercially available xenogenic scaffolds. C-ECM was a fast degrading scaffold that induced a transitional inflammatory

response accompanied by gradual resorption and replacement by host connective tissue in animal models (Burugapalli and Pandit, 2007). Research activities have been carried out to improve the quality and biomaterial properties of C-ECM scaffold by surface modification and functionalization (Chan et al., 2008). Different crosslinking agents were used as a tool for tailoring the properties of C-ECM and the biological stability of C-ECM was maintained by crosslinking with EDC (Burugapalli et al., 2009).

In 2014, Anilkumar, *et al* proposed a new method for isolation of cholecystic ECM that avoided the use of enzymes or detergents and this method significantly improved the biomaterial grade properties of the existing small intestinal submucosa scaffold material (Anilkumar et al., 2014). Isolation procedure for extracellular matrix involved multiple sequential steps including collection of material, decellularization, decontamination, crosslinking and sterilization. Organs or tissues from animal origin are good sources for biomaterial but must undergo proper decellularization. The effect of such chemical treatment affected the biomolecule content and the quality of the scaffold (Fitzpatrick et al., 2010). But in this method of isolation the extensive use of chemical agents for preservation, transportation and decellularization were reduced. In non detergent / enzymatic method formaldehyde was considered as the common fixative as well as the stabilizing agent. This procedure resulted in biomaterial grade scaffolds with a potential clinical application (Anilkumar et al., 2014). Evidences showed that porcine cholecyst derived scaffold prepared by non-detergent/enzymatic method was rich in natural biomolecules like elastin and glycosaminoglycan compared to commercially available porcine small intestinal submucosa derived skin substitute. Studies also showed that this scaffold promoted full thickness wound healing with excess cell proliferation at early phases and acceptable collagen deposition in later phases in rabbit model (Revi et al., 2013). Homologous fibroblast loaded porcine

cholecyst derived scaffold promoted faster healing in full thickness burn wounds in rabbit model by modulating myofibroblast response (Revi et al., 2016). Biocompatibility and immunophenotypic characterization of this scaffold implanted in rat model was studied, compared with SIS, cholecyst derived scaffold was found to be less immunogenic, possessed different immunologic potential and was biocompatible as per ISO standards (Muhamed et al., 2015b).The difference in immunologic potential may be due to the difference in the nature of protein composition and biomolecules based on the source organs used for the preparation of the scaffold. The proteome evaluation study on extractable proteins in porcine cholecyst derived ECM showed a wide distribution of proteins like relevant to graft acceptance, wound healing and tissue remodeling. Some of the proteins present in CDS that promoted wound healing were Caveolin, Decorin, Lumican, Mimecan, Galectin-3, β-2 glycoprotein 1, Nidogen -1 and Nidogen-2 (Muhamed et al., 2015b). This procedure was also suitable for isolation of ECM from hollow organs like urinary bladder and jejenum (Anilkumar et al., 2014). Mass spectroscopic analysis revealed that its rich in diverse set of proteins and growth factors and thereby extending its scope in tissue engineering and regenerative medicine.

MATERIALS AND METHODS

I. Material

Tetrachloroauric acid ($HAuCl_4.\ 3H_2O$) (Sigma), Tri sodium citrate dehydrate (Merck), L-cysteine hydrochloride (Molychem), Glutathione reduced(GSH)(Sigma), Disodium hydrogen phosphate anhydrous (Na_2HPO_4) (Merck), Dimethyl sulfoxide (DMSO),Neutral Buffered Formalin, 35% Hydrochloric acid (Merck),Nitric acid (Merck), Sodium Chloride crystal (Merck), Potassium dihydrogen phosphate(Merck), Fluorescein diacetate (FDA), Propidium Iodide(PI), Sodium dihydrogen phosphate($NaH_2PO_4.7H_2O$) (Merck), N-Hydroxysuccinimide (Molychem), odium bicarbonate(sigma),3-(4, 5-Dimethylthiazol-2-yl)-2, 5-diphenyl tetrazolium bromide (MTT) (Invitrogen), TrypLE (Gibco life technologies), Dulbecco's modified Eagle's medium (DMEM) (Sigma Aldrich), Antibiotic Antimycotic solution (Himedia), 1-Ethyl-3-(3-dimethylaminopropyl)carbodiimide (EDC) (Sigma).

II. Methods

1. Synthesis of Gold Nanoparticles

Gold nanoparticles were synthesized by citrate reduction method by Turkevich (Turkevich et al., 1951)and Frenz. All glasswares and magnetic beads used for synthesis were washed with aqua regia (HCl : HNO_3 in 3:1 dilution) and rinsed 3-4 times with Milli-Q water (Merck Millipore) and oven dried overnight. All the reagents were prepared in Milli-Q water. For the reaction, about 20ml of 0.25mM of Tetrachloroauric acid was boiled at 100°C and added 4ml of 1% Trisodium citrate .This mixture was allowed to boil for about 10 minutes until a cherry red color was obtained resulting in citrate capped gold nanoparticles. Then the colloidal gold solution was cooled at room temperature and centrifuged at 7000rpm, 25°C for 20 minutes (Eppendorf Centrifuge 5430R).The supernatant was removed and the pellet was resuspended in 12ml of

Milli Q water. This solution was filtered using syringe filter of 0.22µm pore size and stored at 4°C for further experiments.

2. Preparation Of Amine Functionalized Gold Nanoparticle

2.1 Cysteine Functionalization Of Gold Nanoparticles

L- Cysteine hydrochloride (Cys) was used to conjugate amine groups to gold nanoparticles. 1mM cysteine was added to 1 ml of gold nanoparticle solution, stirred for 30s and kept at 4°C overnight (Gao et al., 2012).

2.2 Glutathione Functionalization Of Gold Nanoparticles

Glutathione (GSH) was used to conjugate amine groups to gold nanoparticles. 1mM GSH was added to 1 ml gold nanoparticle and stirred for 30s and kept at 4°C overnight (Gao et al., 2012).

3. Characterization Of Citrate Capped Gold Nanoparticles And Amine Functionalized Gold Nanoparticles

3.1 UV-Visible Spectrophotometry Analysis

UV visible spectroscopic measurement was taken by Cary Win100 UV-visible spectrophotometer at 400-800nm range to collect surface plasmon resonance (SPR) of Citrate capped gold nanoparticles (AuNp), Cysteine functionalized gold nanoparticle (Cys-AuNp) and Glutathione functionalized gold nanoparticle (GSH-AuNp).

3.4 Dynamic Light Scattering

The hydrodynamic diameter of nanoparticles, zeta potential and size distribution of the AuNp, Cys-AuNp and GSH-AuNp were determined by Dynamic Light Scattering (DLS, Malvern Nano-ZS). The samples were prepared in 1:10 dilution (100µl gold colloid solution: 1000µl deionized water) and sonicated for 20 minutes at 37°C before DLS measurement. The

hydrodynamic measurement and zeta potential were taken in triplicates, the measured size were presented as average value of 30 runs.

3.3 Environmental Scanning Electron Microscopy

The surface characteristics of gold nanoparticles was noted by Environmental Scanning Electron Microscopy (FEI, Quanta 200, and USA). One drop of nanoparticle solution was dispersed on coverslip and air dried for 10 minutes. The analysis was performed after coating the samples with gold. The samples were observed at an accelerating voltage of 25kV.

3.4 Transmission Electron Microscopy

The morphology, size and shape of the synthesized AuNp, Cys-AuNp and GSH-AuNp were characterized using Transmission Electron Microscopy (Hitachi H-7650) at accelerating voltage of 80kV. The samples for imaging were sonicated in ultrasonic bath sonicator for 15 minutes at 37°C. TEM grids were prepared by drop casting a drop of the gold nanoparticle solution on copper TEM grids and allowed them to air dry for 24 hours and images were taken for analysis.

4. Preparation of Porcine Cholecyst Derived Scaffold

Extracellular matrix (ECM) scaffolds were isolated from porcine cholecyst by an in-house patented procedure (Anilkumar et al., 2014). This method obviated the need for extensive use of detergents and enzymes and resulted in the mechanical recovery of lamina propria after ex situ treatment with a stabilizing agent (10% buffered formalin), which resulted in controlled pre-isolation in situ cross-linking of biomolecules in the scaffold(Revi et al., 2013). It was washed thoroughly in running water for at least 4 hours and the samples were freezed by storing at -80°C and lyophilized overnight for 16 hours. The sheets were cut into discs of 15mm diameter for further experiments and were sterilized by ethylene oxide treatment. This scaffold was used for further experiments and was designated as cholecyst derived extracellular

matrix(C-ECM).

5. Conjugation of Gold Nanoparticle on C-ECM Scaffold:

Gold nanoparticles were incorporated onto porcine cholecyst derived extracellular matrix by two methods; Direct infiltration and chemical crosslinking.

5.1 Direct Infiltration of Gold Nanoparticle on C-ECM Scaffold:

Porcine cholecyst derived scaffold was incorporated with gold nanoparticle by direct infiltration method. Gold colloid solution of 2ml was added to the scaffold and kept on shaking incubator at 37°C for 24 hours. After incubation these scaffolds (AuNp -In CECM) were oven dried at 37°C and stored for further use.

5.2 Chemical Crosslinking of Gold Nanoparticle on C-ECM Scaffold

Cysteine and glutathione modified gold nanoparticles were coupled to porcine cholecyst derived extracellular matrix (C-ECM) scaffolds by EDC-NHS coupling reaction. Both EDC and NHS solutions were prepared in Phosphate Buffered Saline (PBS) and the reaction was carried out at pH 7.4.

Scaffolds were treated with equal volumes of 2 mM EDC and 5 mM NHS, incubated for 30 minutes with shaking for the activation of carboxyl groups. To the reaction mixture 2ml of modified gold nanoparticle solutions were added and kept for incubation respectively and kept for 24 hours incubation. Then the scaffolds were washed in PBS and kept again in shaking incubator for the next 24 hours. Cysteine modified gold nanoparticle conjugated C-ECM (Cys-AuNp CECM) and Glutathione modified gold nanoparticle conjugated C-ECM (GSH-AuNp CECM) scaffolds were oven dried, packed for Ethylene oxide sterilization to perform further experiments (Miyagi et al., 2011).

6. Characterization of Gold Nanoparticle Conjugated Scaffold:

6.1Microarchitecture Analysis By Environmental Scanning Electron Microscopy

The surface morphology of all the three gold nanoparticle incorporated scaffolds were analysed by Environmental Scanning Electron Microscopy as described in section 3.3.

6.2 Energy-Dispersive Spectroscopy

Energy Dispersive X-ray Spectroscopy (EDS) was performed with oxford detector of the above ESEM for elemental composition analysis.

6.3 Fourier Transform Infrared Spectroscopy

The Fourier Transform Infrared Spectra (FTIR) of C-ECM, AuNp-In CECM, Cys AuNp-CECM and GSH AuNp-CECM were recorded in the infra-red range of 2000–400 cm^{-1} using Nicolet 5700 FTIR Spectrophotometer (Nicolet Inc, Madison, USA) by diamond Attenuated Total Reflectance (ATR) method.

6.4 Thermogravimetric Analysis

The Thermogravimetric Analysis was performed using TGA SDT Q600 from TA instruments. The thermal stability of AuNp In-CECM, Cys AuNp-CECM and GSH AuNp- CECM were analyzed. The samples were cut into small pieces of size 3mm, weighed and placed in platinum cups and heated from room temperature to 600°C with heating rate of 10°C /min with calcined alumina as the reference material.

6.5 Evaluation of Gold Nanoparticle Retention on C-ECM Scaffolds

Gold nanoparticle modified scaffolds; AuNp In- CECM, Cys AuNp-CECM and GSH AuNp-CECM were subjected to release study to evaluate the affinity of nanoparticles to the scaffold. The scaffolds prepared by both direct infiltration and chemical crosslinking methods were taken for this study. The scaffolds were immersed in 5ml Phosphate Buffered Saline (PBS)

solution and kept at 37°C in shaking incubator. 2ml of the solution was collected at every 12 hours and replaced with fresh PBS solution. The samples were analysed using UV visible spectrophotometer for the presence of gold nanoparticles. The experiment was performed for 7 days and observations were made.

6.6 Conductivity of the Scaffolds

Conductivity was measured using Digital Multimeter (Mastech MAS830L Digital Multimeter). Phosphate buffer saline hydrated scaffolds with a thickness of 0.2 mm and a diameter of 15 mm were placed inside the vacant space between the two probes. Resistance measurement (R) was carried out for three specimens of each sample and the conductivity (δ) was calculated by Pouillet's law equation (Shahini et al., 2013).

$$\sigma = L/(R*A)$$

where L is thickness, D is diameter of the scaffold, and A is the surface area of scaffold, $A = \pi \times (D/2)2$. The obtained values for conductivity were expressed in micro Siemens / millimetre (µS/mm).

7. Biological Evaluation of Scaffolds

7.1 Standardization of Cell Culture and Maintenance of H9c2 cell line

General cytotoxicity and cytocompatability of Cys AuNp-CECM and GSH AuNp-CECM was assessed by culturing cardiomyoblast cells; H9c2 purchased from NCCS, Pune, India. The fabricated scaffold was intended for cardiac tissue engineering applications, hence cardiomyoblast cell line was selected to envisage its biocompatibility. The cells were maintained in Dulbeccos Modified Eagles Medium (DMEM) with high glucose and supplemented with 10% Fetal Bovine Serum (FBS) and 1% Antibiotic Antimycotic solution at 37 °C in a CO_2 incubator set at 99 % relative humidity and 5% CO_2. Confluent cells in the cell

culture flask were washed twice with 1 ml Phosphate Buffered Saline (PBS) and treated with 1 ml TrypLE solution and placed at 37°C in CO_2 incubator set at 99% relative humidity and 5% CO_2 for 2-3 minutes allowing the cells to detach from the surface. Once the cells were detached from the cell culture flask, the TrypLE present in the flask was inactivated using DMEM containing 10% FBS. The cells were then centrifuged at 3000 rpm for 5 minutes and the pellet was resuspended in the same medium mentioned above. Trypan blue exclusion staining of the cell suspension was carried out and viable cells were counted by heamocytometer. The cells were incubated in CO_2 incubator at 37°C with 5% CO_2 and 99% humidity. Media change in cell culture flasks were carried out every 2-3days. Cryopreservation was done by treating the cell suspension in whole serum containing 10% DMSO (Dimethyl sulphoxide). Cytotoxicity was evaluated by direct contact test and test on extract method. Cytocompatability of cysteine capped gold nanoparticle conjugated porcine cholecyst derived extracellular matrix (Cys AuNp – CECM) and glutathione capped gold nanoparticle conjugated porcine cholecyst derived extracellular matrix (GSH AuNp-CECM) for cardiac tissue engineering were analyzed by cell adhesion, cell viability and proliferation.

7.2 Cytotoxicity Assessment

7.2.1 Cytotoxicity by Direct Contact Test

The cytotoxicity of Cys AuNp – CECM and GSH AuNp – CECM were tested by direct contact method (ISO 10993-5) (Prasad et al., 2015). 1 x 10^5 cells were seeded in 24 well plate and maintained for 3 days. After attaining 80% confluency, the culture medium was removed and the scaffolds of size 4mm were placed carefully on the cell monolayer. This was incubated for 24 hours after the addition of sufficient culture medium. Cytotoxicity was determined by assessing the morphology, detachment and lysis of cells by using inverted phase contrast microscope. The

viability of cells after direct contact test was also assessed by treating with neutral red dye. The stock solution of neutral red was made in distilled water (1mg/ml). Prior to use, the working solution was prepared in 1.8% NaCl (1:1 dilution). 500µl neutral red solution was added to each well and incubated for 10 minutes at 37°C. Then the wells were washed with Phosphate Buffered Saline (PBS) 2-3 times and observed under inverted phase contrast microscope (Prasad et al., 2015).

7.2.2 Cytotoxicity by Test on Extract

Extracts of Cys AuNp-CECM and GSH- AuNp CECM were obtained by incubating the scaffolds in 1ml DMEM containing 10% FBS at 37°C with continuous shaking for 24hours. The extracts were obtained and added to subconfluent H9c2 cells ($1x10^6$ cells) and incubated at CO_2 incubator with 99% relative humidity, 5%CO_2 and 37°C for 24 hours. Cells cultured in DMEM medium was taken as the control. After incubation, the medium as well as the extract was removed and 50 µl MTT reagent (0.5mg/ml) was added and incubated for 3 hours at 37°C in a CO_2 incubator allowing the formation of formazan crystals. After incubation 500µl Dimethyl sulphoxide (DMSO) was added and kept for 2 hours protected from light for solubilizing the formazan crystals. Absorbance was taken at 570 nm in a multiwell plate reader (Biotech Synergy 4, USA). The percentage viability was calculated using the formula,

Viability in percentage = (OD of test/ OD of control) ×100

Percentage cell viability of 80% or above was considered as viable.

7.3 Cytocompatability Assessment

7.3.1 Live and Dead Staining

The viability of cells on Cys AuNp–CECM and GSH AuNp-CECM was determined by staining with Fluorescein Diacetate (FDA) and Propidium Iodide (PI). All reagents were freshly prepared.

The stock solution of FDA was prepared in acetone (10mg/ml). On prior to use 10µl of FDA was made upto to 1ml using serum free media. 1x 10^5 cells were seeded on the scaffolds and kept in CO_2 incubator for 2-3 days. The cell seeded scaffolds were treated with 500µl FDA for 10 minutes and added 100µl of PI (10mg/ml) and incubated for 30 seconds and examined under fluorescence microscope.

7.3.2 Cell Proliferation Assay

Cell proliferation study on scaffold was assessed by MTT assay at the end of 3rd and 7th day. 1x 10^5 cells were seeded on Cys AuNp–CECM and GSH AuNp-CECM and incubated on CO_2 incubator. Cells cultured in DMEM medium was taken as the control. After incubation the medium was removed and 50 µl MTT reagent (0.5mg/ml) was added and incubated for 3 hours on CO_2 incubator with 99% relative humidity, 5%CO_2 and 37°C allowing the formation of formazan crystals. After incubation 500µl Dimethyl sulphoxide (DMSO) was added and kept for 2 hours protected from light for solubilizing the formazan crystals. Absorbance was taken at 570 nm in a multiwell plate reader (Biotech Synergy 4, USA). The percentage viability was calculated using the formula,

Viability in percentage = (OD of test/ OD of control) ×100

Percentage cell viability of 80% or above was considered as viable.

RESULTS AND DISCUSSION

1. Synthesis Of Gold Nanoparticles

The synthesis of gold nanoparticles were carried out by chemical reduction of Tetrachloroauric acid solution using Trisodium citrate as the reducing agent, stabilizing agent as well capping agent as proposed by Turkevich (Turkevich et al., 1951) and Frens. When Trisodium citrate solution was added to the boiling Tetrachloroauric acid, instantaneous colour change from pale yellow to cherry red colour was observed, which indicated the reduction of gold ions (Au^{3+}) to gold atoms (Au^{+}) Fig.3.

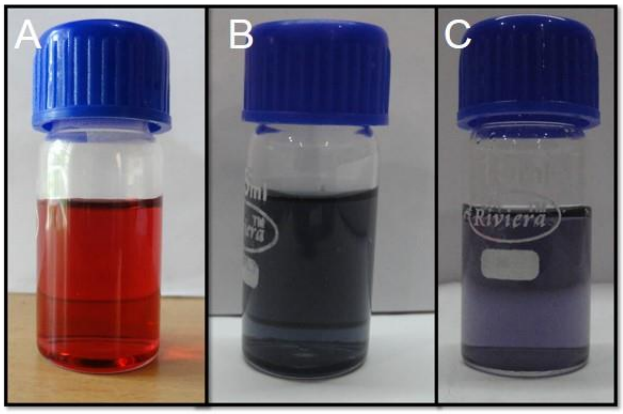

Fig.3 Photographs of cherry red coloured gold colloid solution (A), blue coloured Cys-AuNp (B) and purple coloured GSH AuNp (C).

The colour change confirmed the presence of citrate capped gold nanoparticle which was due to the surface plasmon resonance of gold nanoparticle. This method of gold nanoparticle synthesis resulted in the formation of negatively charged citrate ions on nanoparticle surface by weak bonds. This layer provided long term stability and monodispersity by electrostatic repulsive forces (A. Rajeshwari, 2015). In fact, the layer of citrate ions are displaceable with other compounds like amines, thiols containing compounds, proteins, peptides, antibody and polymers for the functionalization of nanoparticle as per the required application (Dobrowolska

et al., 2015; Gao et al., 2012).

2. Preparation Of Amine Functionalized Gold Nanoparticle

Surface of the synthesized citrate capped gold nanoparticle was modified with thiol containing compounds; L-Cysteine (Cys) and Glutathione (GSH) by chemisorption process. The amount of cysteine required for functionalizing gold nanoparticle was standardized by varying cysteine concentration. 200µl of 1mM cysteine solution was the optimum concentration for amine functionalization. The process was confirmed by the color change from cherry red color of gold colloid solution to blue colour (Aryal et al., 2006) (Fig. 3). For amine functionalization using glutathione, 500µl 1mM glutathione was found to be the optimum concentration. A change in colour from cherry red colour to purple confirmed the capping of gold nanoparticles with GSH (Mao et al., 2010) (Fig. 3). The colour change observed was due to the aggregation of particles by the replacement of stabilizing citrate layer of synthesized gold nanoparticle with Cys and GSH.

L-cysteine is an amino acid with a thiol group (-SH) on the side chain. This thiol group bind to Au+ formed by synthesis and are resulted in Au-S bonds. Glutathione is a tripeptide molecule with a central cysteine thiolate for covalent attachment to the gold nanoparticle surface. Thiol groups of these compounds are covalently attached to gold nanoparticle surface by Au-S bond, thereby increasing the stability and dispersity of gold nanoparticle in aqueous solutions. When the inter-particle distance in the aggregates decreases to less than about the average particle diameter, the electric dipole–dipole interaction and coupling between the plasmons of neighboring particles in the aggregates results in the bathochromic shift of the absorption band (Wang et al., 2013).

3. Characterization of Gold Nanoparticle and Amine Functionalized Gold Nanoparticles

3.1 UV visible Spectrophotometric Analysis

The presence of gold nanoparticle was confirmed by UV visible absorbance measurement and the synthesized gold nanoparticle showed an intense surface plasmon resonance absorption band at 523 nm which was the characteristic peak of gold nanoparticles (Mohamed Anwar K Abdelhalim, 2012). Gold nanospheres exhibited a single absorption peak in the visible range from 510-550nm due to the surface plasmon resonance. This heavy absorption peak at 520nm gives a red colour to gold nanoparticle solution and changed according to their size.

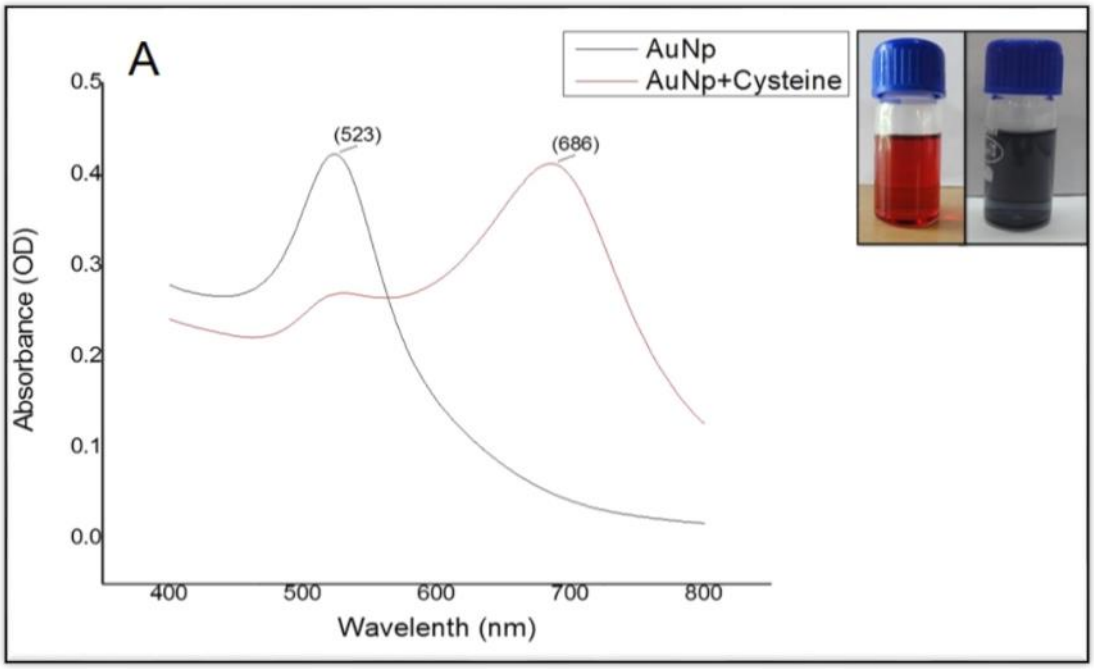

Fig .4A UV visible spectra of Cysteine capped gold nanoparticle (Cys- AuNp)

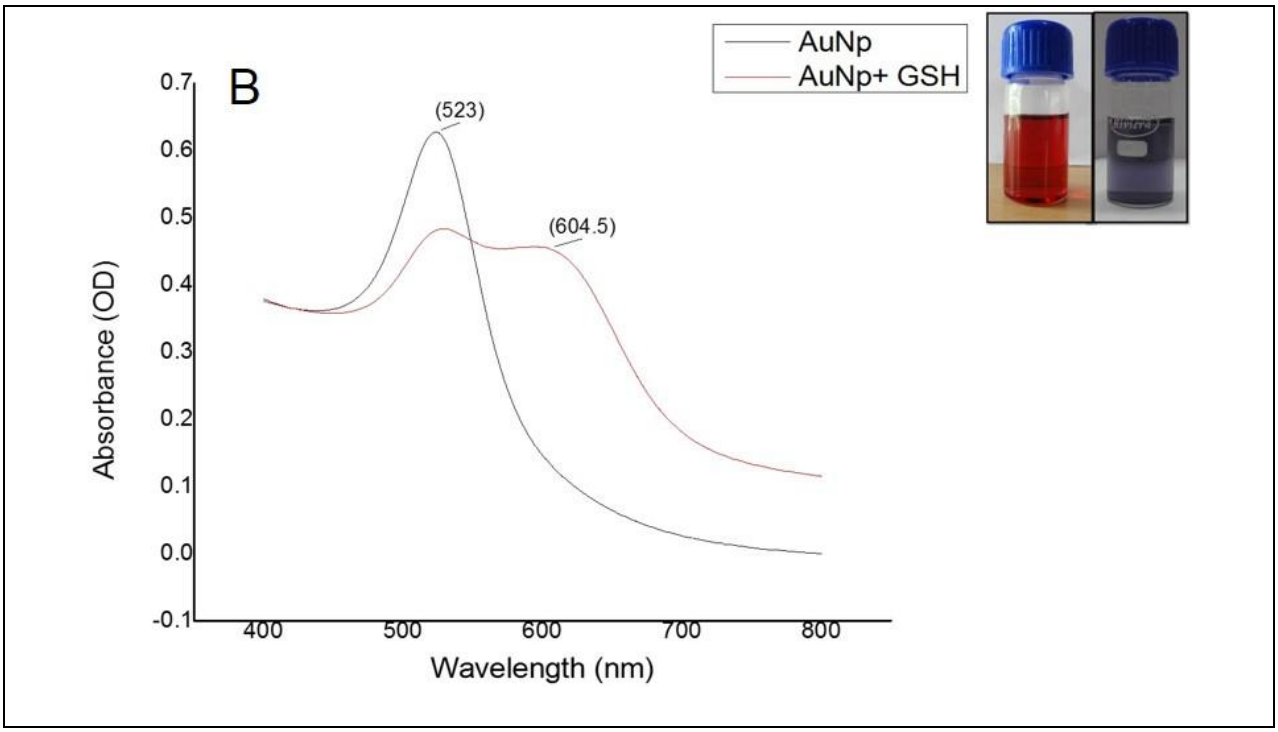

Fig. 4B UV visible spectra of Glutathione capped gold nanoparticle (GSH-AuNp)

UV visible spectra of Cysteine capped gold nanoparticle (Cys- AuNp) showed two peaks; the first distinct peak at 523 nm which was the original absorption maxima of bare gold nanoparticle and second broad new peak at 623 nm (Fig.4A) This peak at longer wavelength is certainly due to the coupling of surface plasmon resonance of adjacent gold nanoparticles and is an indication of the anisotropic optical properties of the gold nanoparticles aggregation and formation of cysteine capped gold nanoparticles were confirmed (Wang et al., 2013). Cysteine stimulates the aggregation of AuNps through the formation of inter-particle H-bonds and zwitterionic electrostatic interactions (Hormozi-Nezhad et al., 2012a). UV visible spectra of Glutathione capped gold nanoparticle (GSH-AuNp) also showed a peak at longer wavelength; 604 nm, is due to aggregation of particles, which confirmed modification of gold nanoparticle with glutathione (Fig.4 B). Displacement of the citrate group on AuNp surface with thiol compounds, such as cysteine and glutathione, induces the aggregation process, due to the

hydrogen bonding or electrostatic interaction between non-covalently adsorbed thiol compounds.

3.2 Dynamic Light Scattering

The results obtained from UV visible spectra confirmed the presence of gold nanoparticle and amine functionalization. Further characterization of AuNp, Cys-AuNp and GSH-AuNp were analysed by Dynamic light scattering. The hydrodynamic diameter, zeta potential and size distribution of these particles were analysed. Three cycles of different counts were performed for analysis of hydrodynamic diameter or particle size and zeta potential. The average mean of these counts were used to confirm the particle size and diameter. The average diameter of bare AuNp or citrate capped gold nanoparticle obtained from DLS was found to be 30nm.

Zeta potential measurement is a key parameter in characterization of gold nanoparticles. Electrostatic interactions in particle dispersions is important in determining the stability of colloidal dispersions (Kaszuba et al., 2010). In the present study, the Zeta potential of AuNp was found to be highly negative; -51.5mV (Fig.5A). This highly negative value is probably due to the citrate ions capped on gold nanoparticle surface. Upon addition of Cys and GSH for amine functionalization of AuNp, changes were observed both in particle size as well as in zeta potential. The average diameter of Cys-AuNp and GSH-AuNp were found to be 223.8nm and 118.4nm respectively.

Dynamic light scattering measures the Brownian motion of a particle and derive the hydrodynamic diameter (Hinterwirth et al., 2013). The increase in the size of particles upon functionalization was due to the aggregation of nanoparticles by modification with cysteine (Aghajanloo et al., 2015) and glutathione (Hormozi-Nezhad et al., 2012b). The zeta potential values of Cys-AuNp and GSH-AuNp were increased, -23.5 mV and -12.5mV respectively.

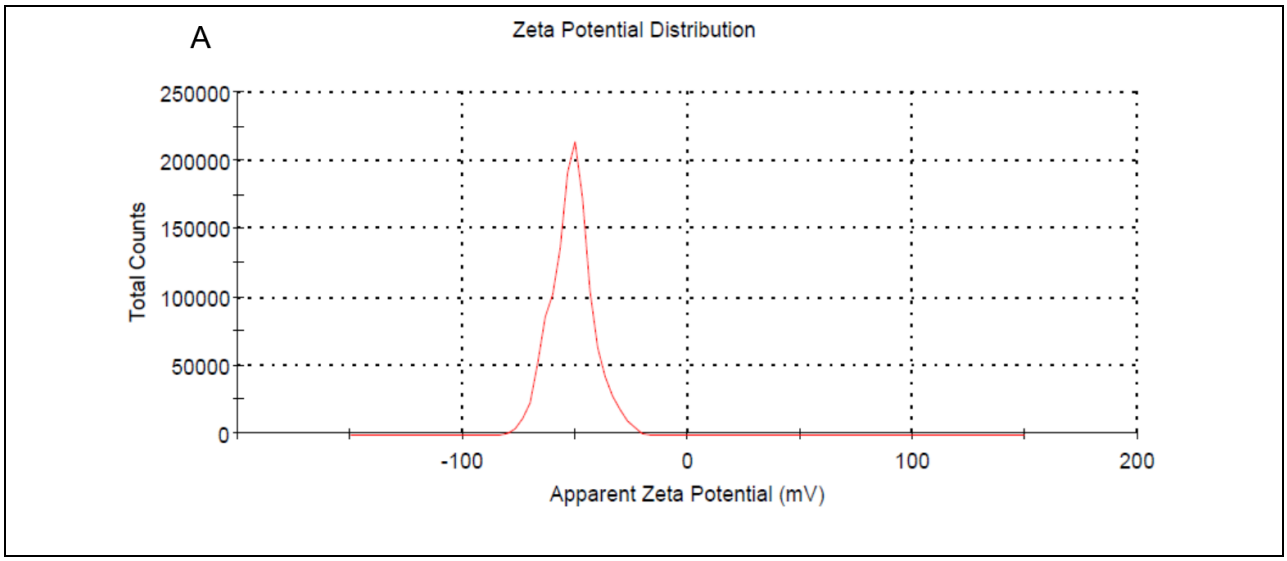

Fig .5A Zeta potential distribution graph of citrate capped gold nanoparticles

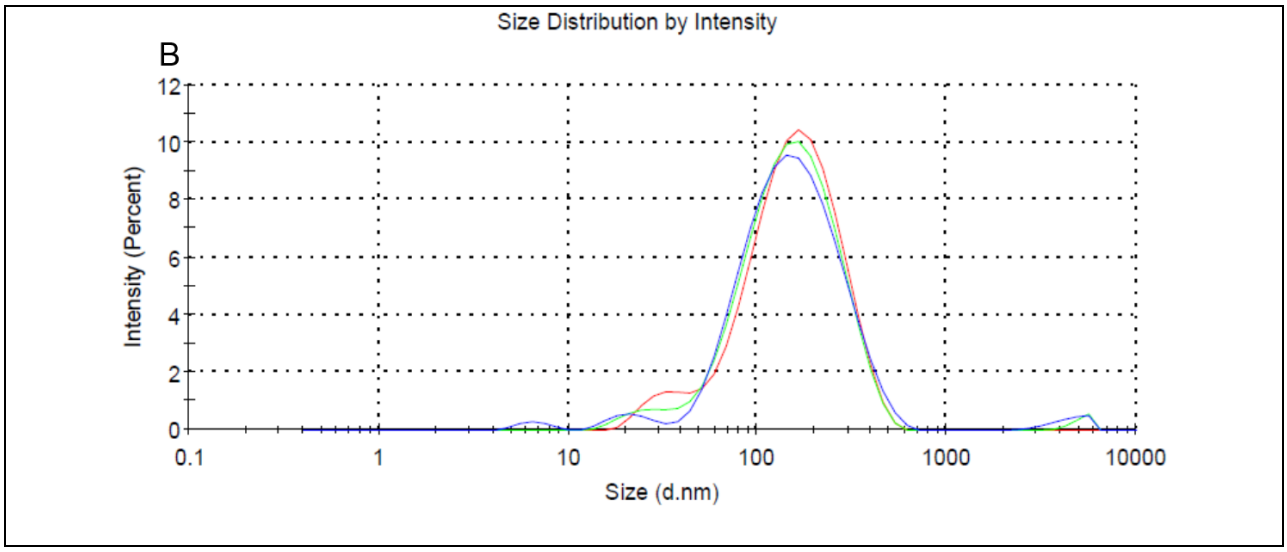

Fig .5B Size distribution graph of Cys-AuNp

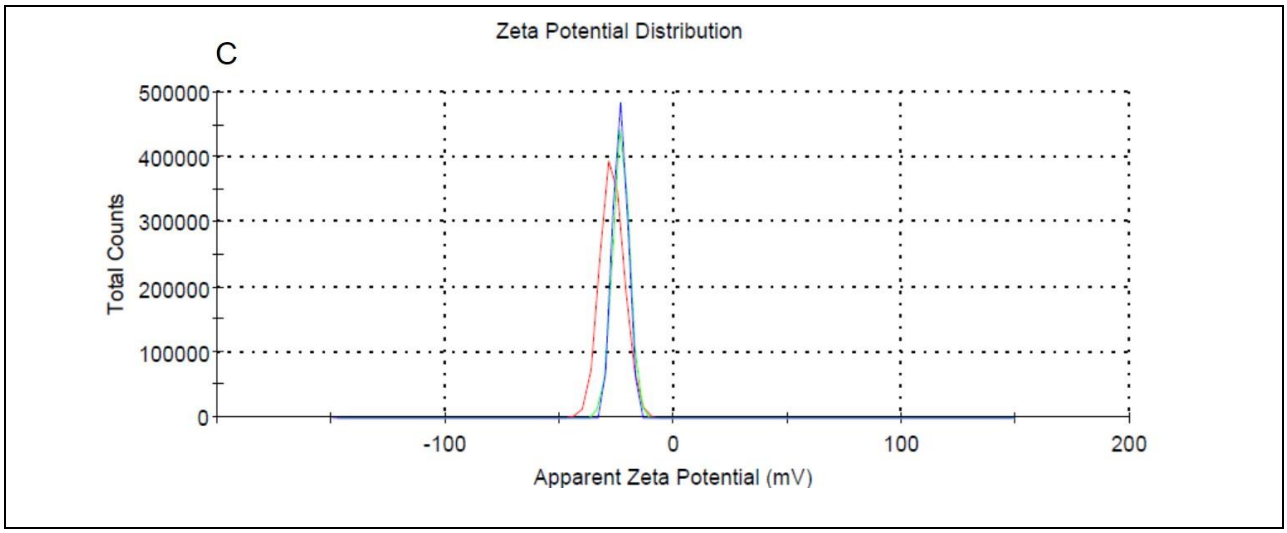

Fig. 5C Zeta potential distribution graph of Cys-AuNp

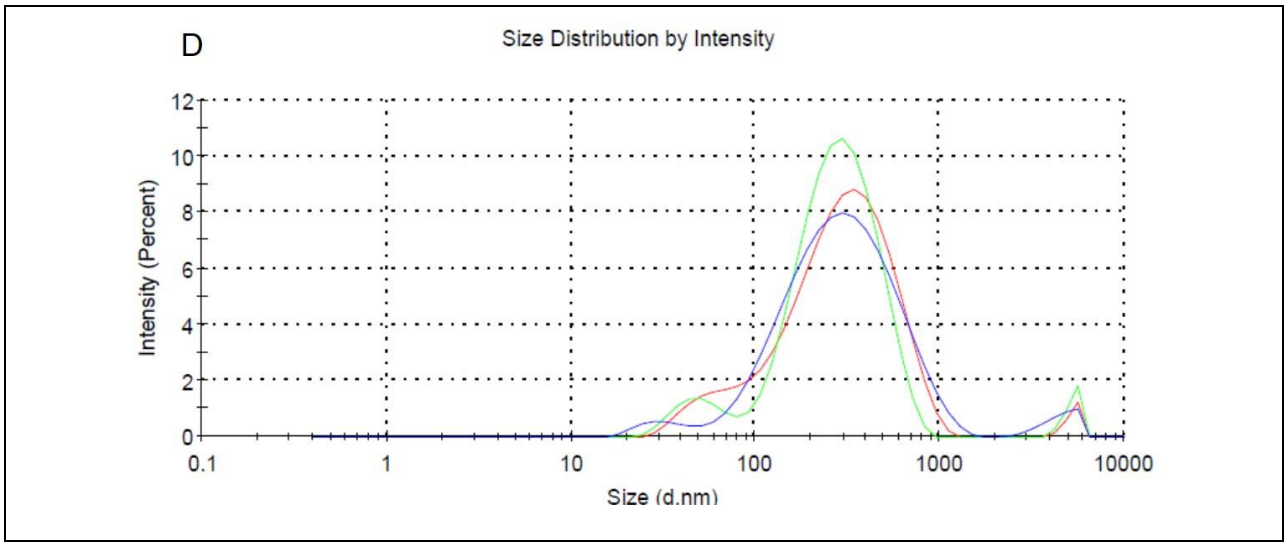

Fig .5D Size distribution graph of GSH-AuNp

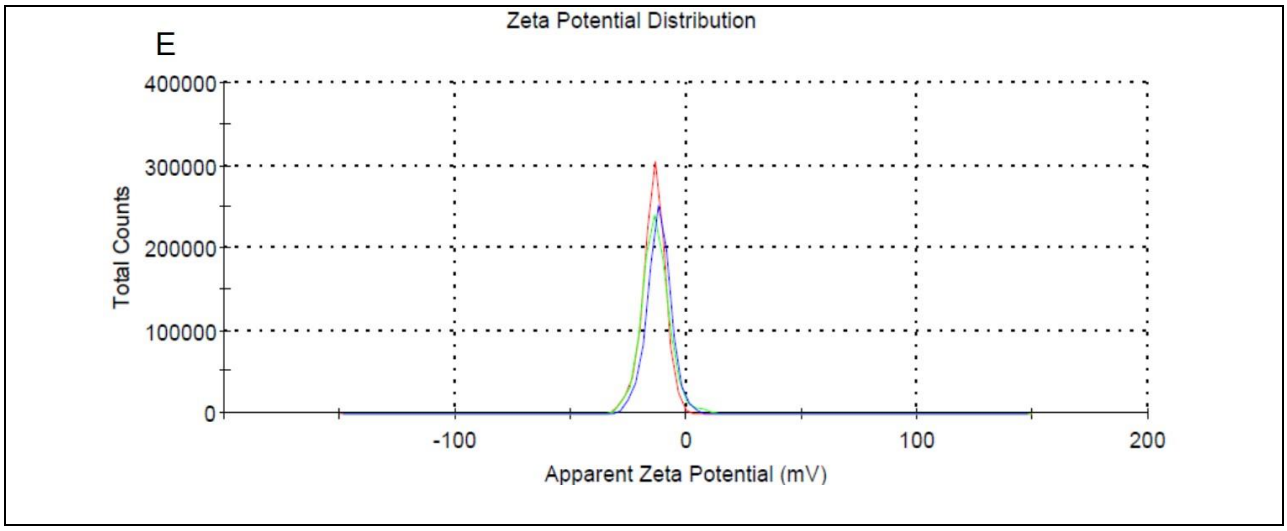

Fig .5E Zeta potential distribution graph of GSH-AuNp

3.3 Environmental Scanning Electron Microscopy

The DLS data showed the average size and stability of gold nanoparticles. With the effort to analyze the shape and surface characteristics of gold nanoparticles, Environmental scanning electron microscopy was performed. The Electron micrographs of gold nanoparticles before and after amine functionalization are shown in Fig.6.

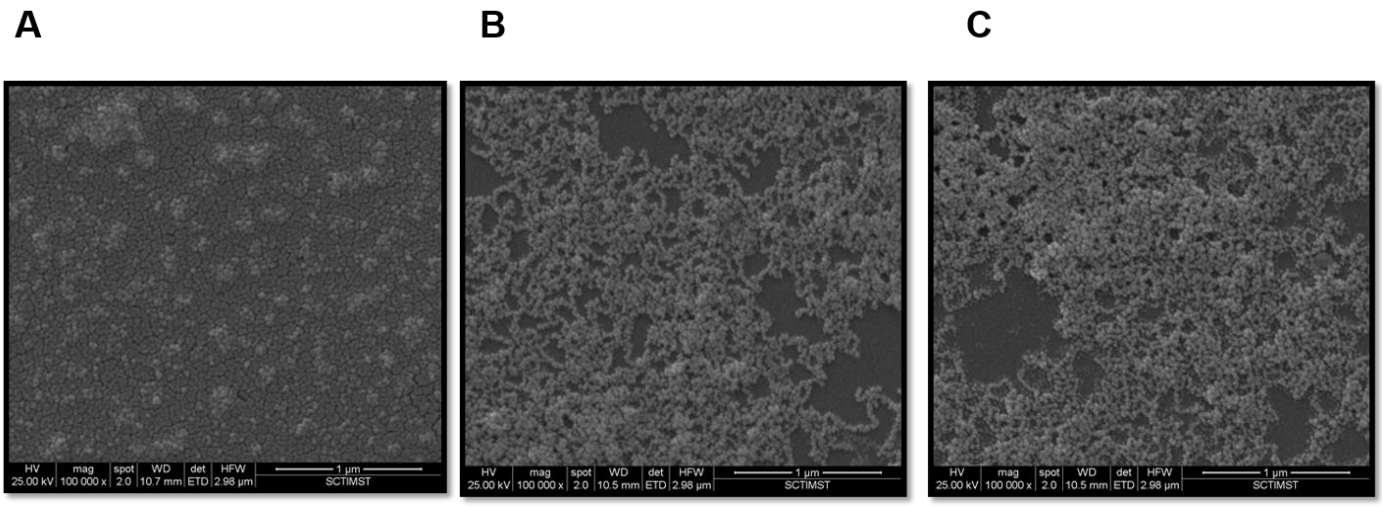

Fig.6 ESEM images of AuNp (A), Cys - AuNp (B) and GSH-AuNp (C)

The surface morphology and aggregation characteristics of bare gold nanoparticles, Cysteine capped gold nanoparticle and Glutathione capped gold nanoparticle were analyzed. Spherical and

dispersed structures were observed in bare AuNp whereas the particles were found attached to each other in Cys-AuNp and GSH–AuNp. This observation clearly indicated the aggregation of gold nanoparticles after cysteine and glutathione addition.

3.4 Transmission electron microscopy

Relative shape and surface morphology of gold nanoparticles were analyzed by ESEM as described above. Further, the size, shape and morphology of synthesized gold nanoparticle were corroborated by TEM (Fig.7). Electron micrographs showed that most of the particles were spherical in shape and the gold colloid solution was monodisperse.

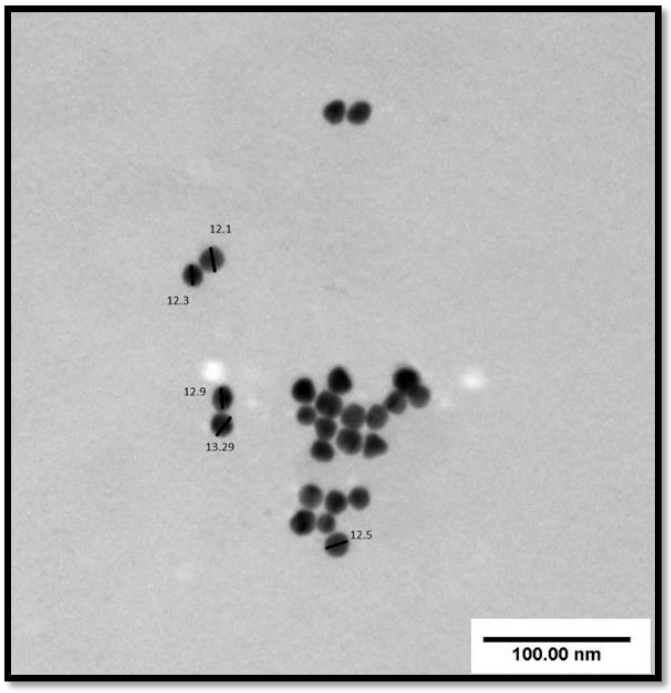

Fig.7 TEM image of gold nanoparticles

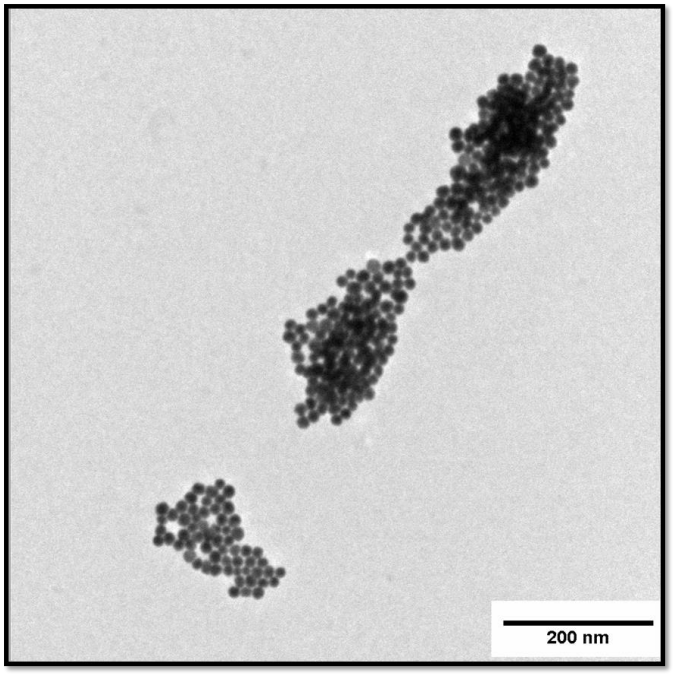

Fig.8 TEM image of Cys-AuNp

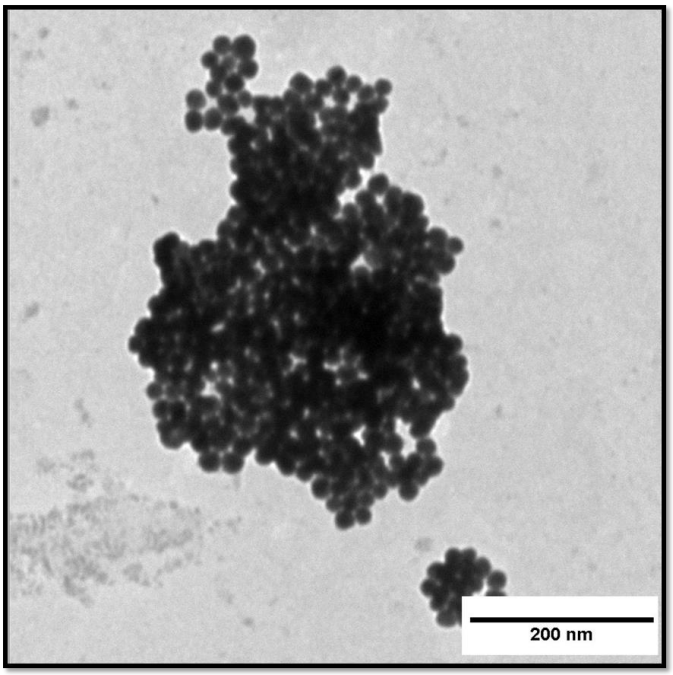

Fig.9 TEM images of GSH-AuNp

The size of the gold nanoparticle was measured by Image J software and the average size obtained was less than 15 nm (Fig 7). Transmission electron microscopic images of Cys-AuNp showed chain like arrangement of particles (Fig.8). The -SH group of cysteine binds to the surface of nanoparticles and this Cys-AuNps are bound to each other by the electrostatic interaction between the protonated amino group and deprotonated carboxy moiety (Sarangi et al., 2009).GSH is also attached to gold nanoparticles by -SH group linkage and are bound to each other by hydrogen bonding strategy (Hormozi-Nezhad et al., 2012b). TEM images of GSH-AuNp confirmed the successive aggregation of gold nanoparticles after capping with GSH (Fig.9).

4. Preparation of Porcine Cholecyst Derived Scaffold And Gold Nanoparticle Conjugation:

Porcine choleyst derived extracellular matrix (C-ECM) was prepared as per the protocol (Anilkumar et al., 2014) described from the host laboratory. Isolated scaffold was lyophilized overnight, stored in dessicator and used for further experiments (Fig.10). The scaffold was then successfully conjugated with gold nanoparticles by EDC/NHS chemistry.

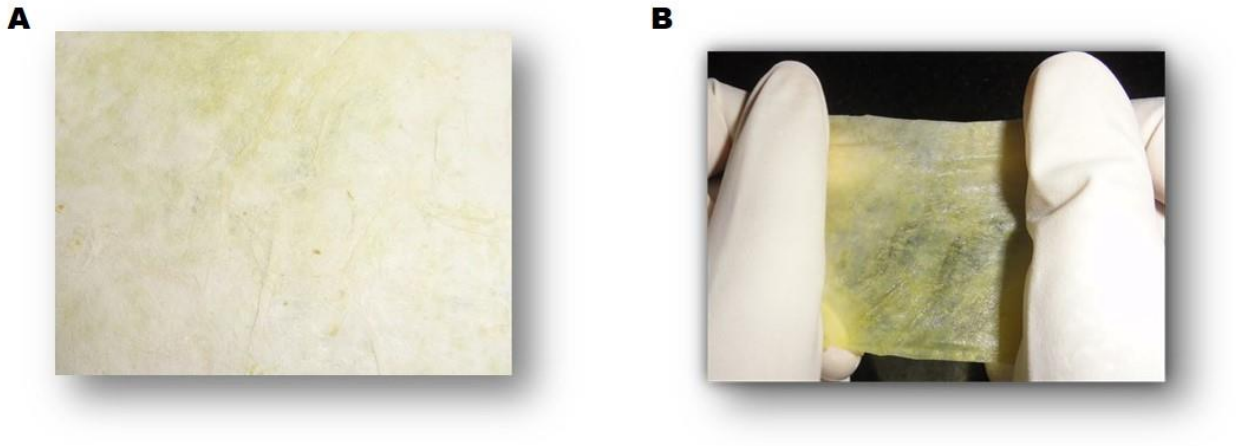

Fig. 10 Photographs of porcine cholecyst derived extracellular matrix, Lyophilized (A) and hydrated (B)

Porcine cholecyst derived extracellur matrix is comprised of different proteins and has been found to be less immunogenic (Muhamed et al., 2015c) as well as a potential scaffold for wound healing application (Revi et al., 2013). C-ECM is rich in collagen proteins, the carboxyl groups of these proteins are bound to the amino group of gold nanoparticle modified with thiol compounds; cysteine and glutathione. In the present instance thiol compounds were used to functionalize gold nanoparticles so that they could easily bind with the carboxyl group of proteins in the C-ECM, through peptide bonds. Crosslinking of gold nanoparticles with C-ECM was performed by 1-ethyl-3-(3-dimethyl aminopropyl) carbodiimide (EDC) and N-hydroxysuccinimide (NHS) chemistry. EDC is the most commonly used carbodiimides for aqueous crosslinking. EDC reacts with carboxyl groups and forms an active intermediate (O-acylisourea) which can be easily displaced by nucleophilic attack from the amino groups in the reaction mixture and results in peptide bond formation. In the present study, considering that unstable the intermediate compound and the probability for hydrolysis, NHS was added along with EDC to improve the stability of intermediates. It is known that, EDC helps in coupling of NHS to carboxyl groups resulting in the formation of NHS ester which is more stable than the intermediate O-acylisourea. EDC and NHS chemistry thus resulted in successful conjugation of gold nanoparticles on C-ECM and this was confirmed by different characterization techniques (Duan and Sheardown, 2005).

5. Characterization of Gold Nanoparticle Conjugated Scaffold:

Gold nanoparticles were conjugated onto C-ECM by both direct infiltration and chemical crosslinking method. Direct infiltration method involved the direct treatment of C-ECM with AuNp solution. Chemical crosslinking of gold nanoparticle on C-ECM involved EDC/NHS chemistry as mentioned before. Cysteine capped gold nanoparticle (Cys-AuNp) and Glutathione

capped gold nanoparticle (GSH-AuNp) were coupled with C-ECM and characterized by different methods mentioned below.

5.1 Microarchitecture Analysis by Environmental Scanning Electron Microscopy

Environmental Scanning Electron Microscopy was performed to study the surface morphology and structural analysis of C-ECM (Fig.11) and of gold nanoparticle conjugated C-ECM. ESEM images of Cys AuNp-CECM (Fig.13) and GSH AuNp-CECM (Fig.14) showed thick fibrous and uniform structure due to the chemical cross linking of gold nanoparticle.

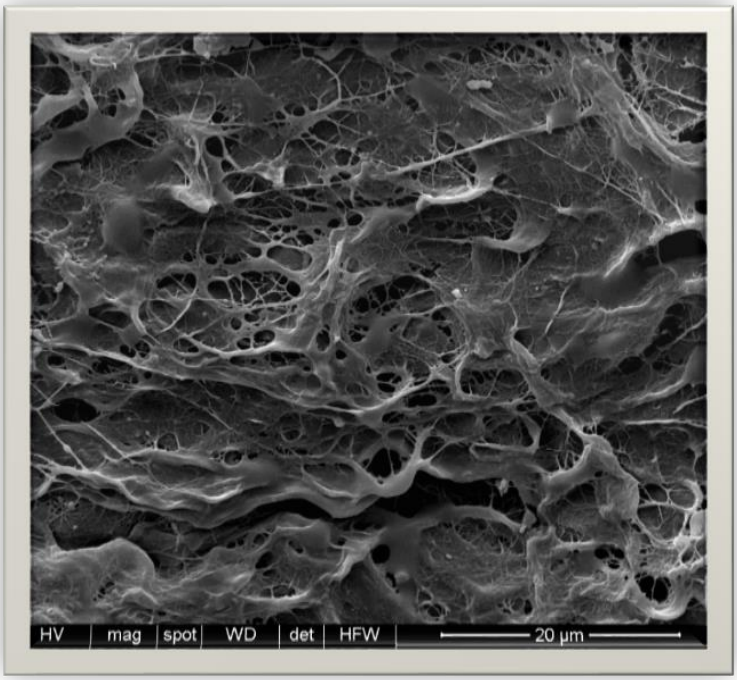

Fig.11 ESEM image of C-ECM

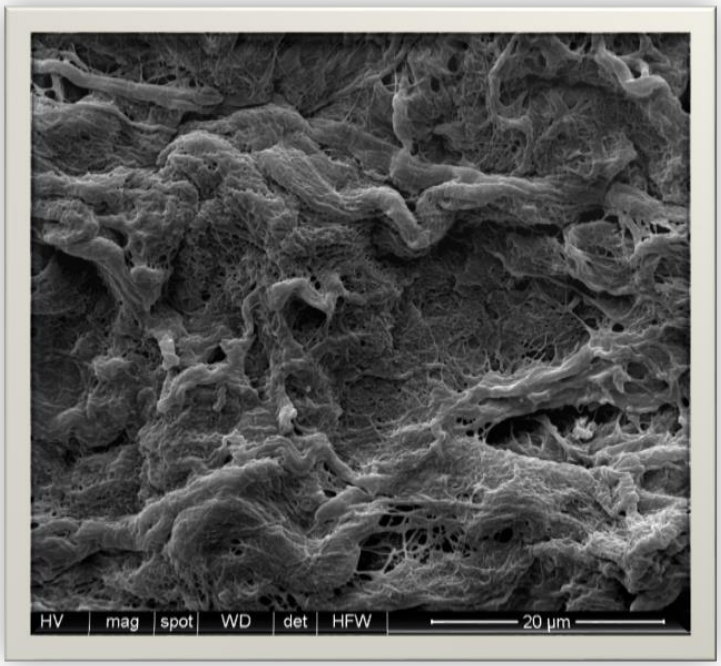

Fig.12 ESEM image of AuNp-In CECM

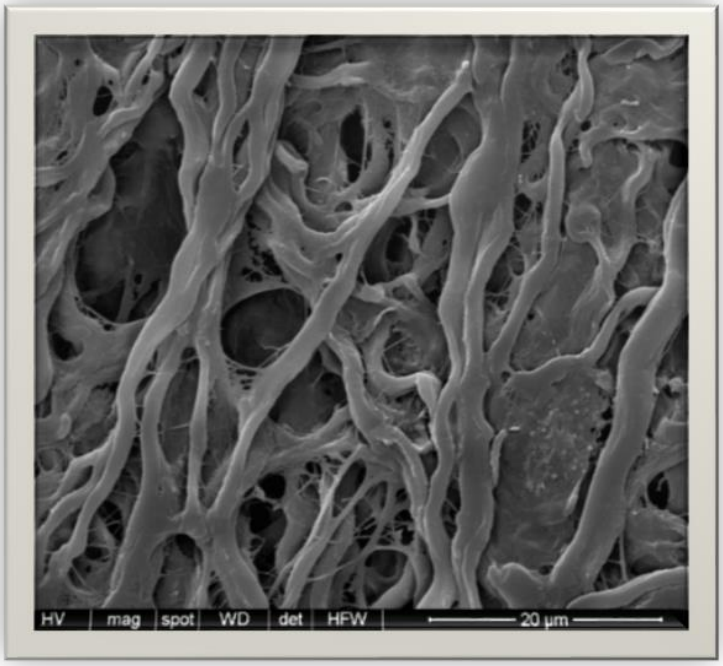

Fig.13 ESEM image of Cys-AuNp CECM

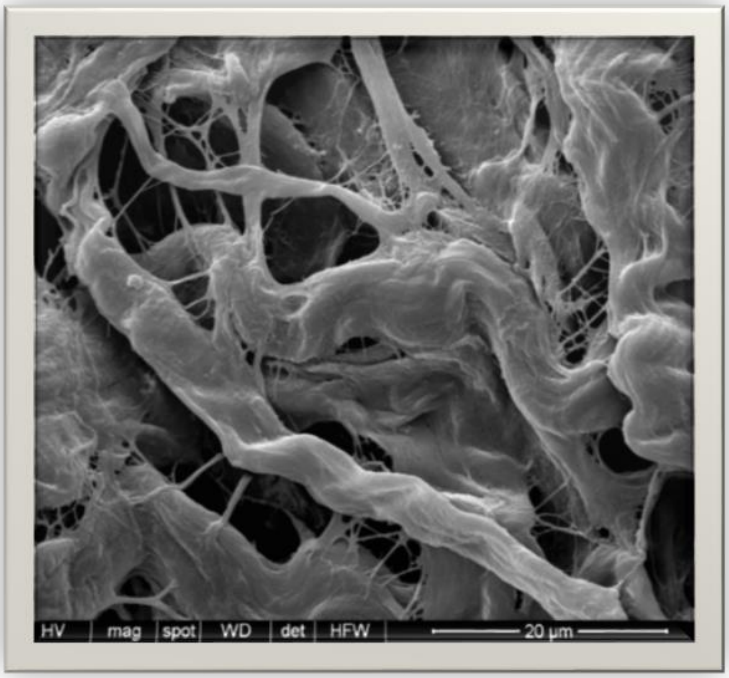

Fig. 14 ESEM image of GSH- AuNp CECM

The fibres were found to be thin in C-ECM while was much denser AuNp-In CECM. (Fig. 12).This confirmed the presence of well-preserved collagen molecules on scaffold even after the incorporation of gold nanoparticles. But in the case of AuNp In CECM, dense and rough surface morphology was observed (Fig.12). It was confirmed that even after the processing steps of gold nanoparticle conjugation, the microarchitecture was maintained.

5.2 Energy-Dispersive Spectroscopy

Scanning Electron Microscopy-Energy Dispersive Spectroscopy was performed for elemental analysis of the scaffold and there by confirming the incorporation of gold nanoparticles on the scaffolds. No traces of gold were found in C-ECM and AuNp In CECM (Fig.15).Thus it was concluded that, in AuNp-In CECM prepared by direct infiltration method gold nanoparticles were not conjugated.

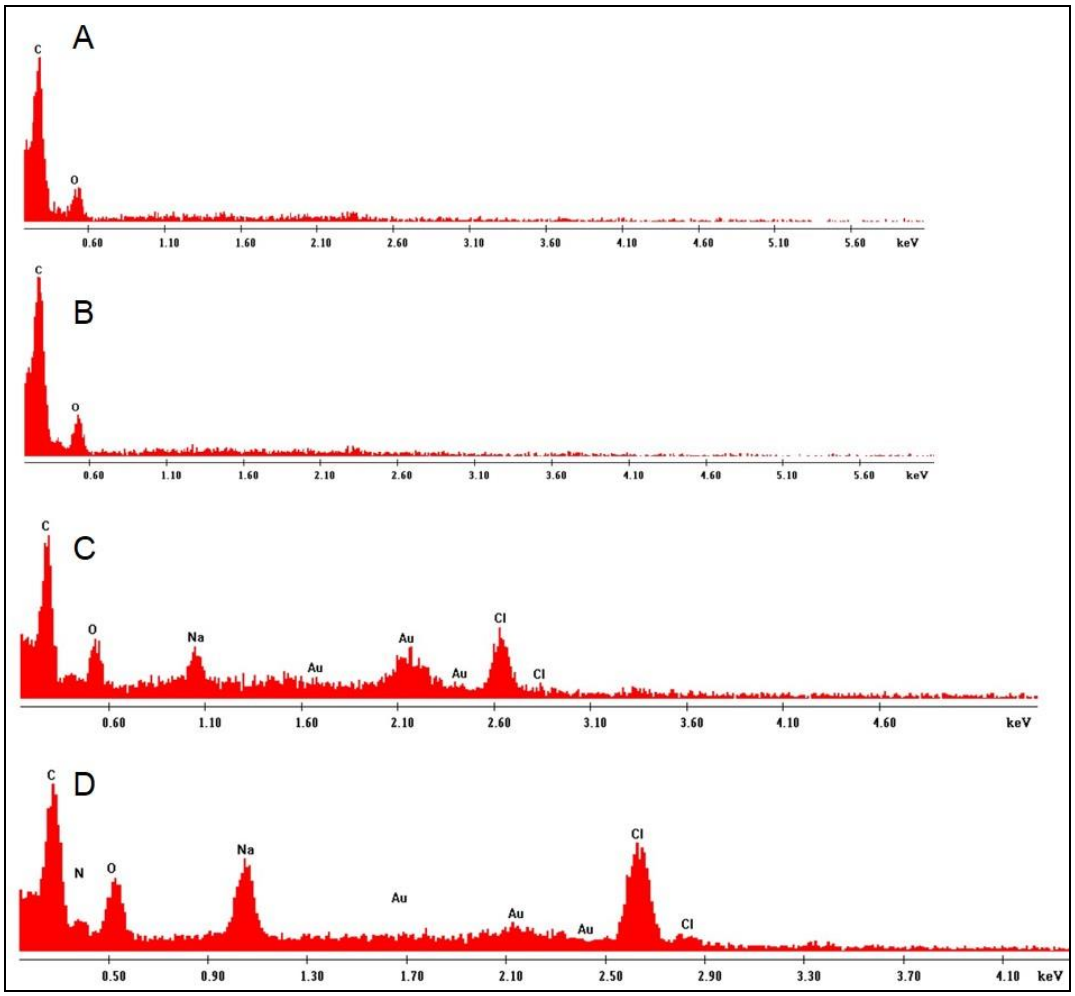

Fig.15 Elemental analysis by SEM-EDS of C-ECM (A), AuNp In CECM (B), Cys AuNp-CECM (C) and GSH AuNp-CECM (D)

Gold nanoparticle did not get coupled with the scaffold when attempted by direct infiltration method of conjugation and the method was found inappropriate. Traces of gold were found in both Cys-AuNp CECM and GSH-AuNp CECM (Fig.15) which was conjugated by EDC/NHS chemistry. Thus, EDS confirmed the successful conjugation of gold nanoparticles onto the scaffold Traces of sodium and chlorine were also found in these scaffolds due to PBS washing done to remove the crosslinking solution. Since there was no evidence for gold nanoparticle conjugated on AuNp In CECM, this scaffold was not considered for further experiments.

5.3 Fourier Transform Infrared Spectroscopy

Fourier Transform Infrared Spectroscopy was performed to analyse characteristic peaks in the scaffolds before and after gold nanoparticle incorporation.

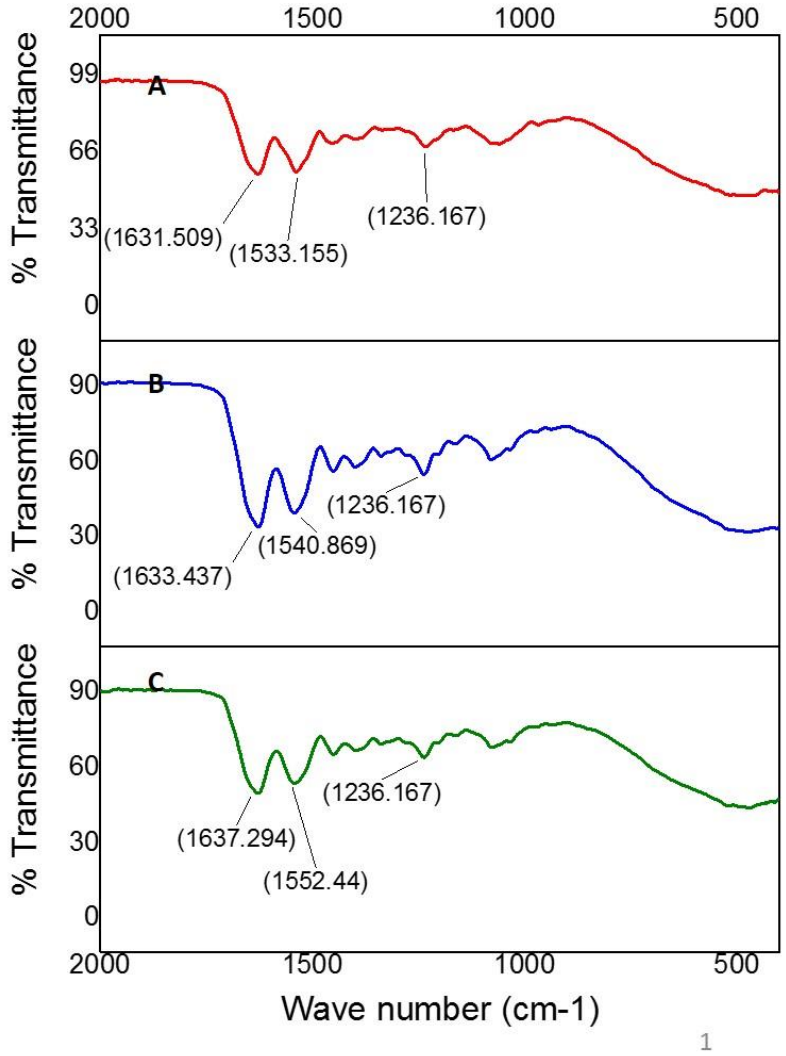

Fig.16 Characteristic collagen peaks of C-ECM (A.), Cys AuNp-CECM (B) and GSH AuNp-CECM (C)

This is a vibrational spectroscopic technique that takes advantage of asymmetric molecular stretching, vibration, and rotation of chemical bonds as they are exposed to designated

wavelengths of light. Fourier transform is to transform the signal from the time domain to its representation in the frequency domain. Characteristic collagen peaks(Movasaghi et al., 2008) at 1631(amide I), 1533 (amide II) and 1236 (amide III) were observed in C-ECM, Cys AuNp-CECM and GSH AuNp-CECM (Fig.16). The observations confirmed that even after the conjugation of gold nanoparticle on C-ECM, collagen proteins on the scaffold were preserved. The myocardial matrix mainly consists of type I and type III collagens (Venugopal et al., 2012) which mimics C-ECM.

5.4 Thermogravimetric Analysis

Thermogravimetric analysis (TGA) measures the change in amount and rate of weight change of a material during heating. Thermograms of C-ECM, Cys AuNp-CECM and GSH AuNp-CECM were analyzed as depicted in Fig.17

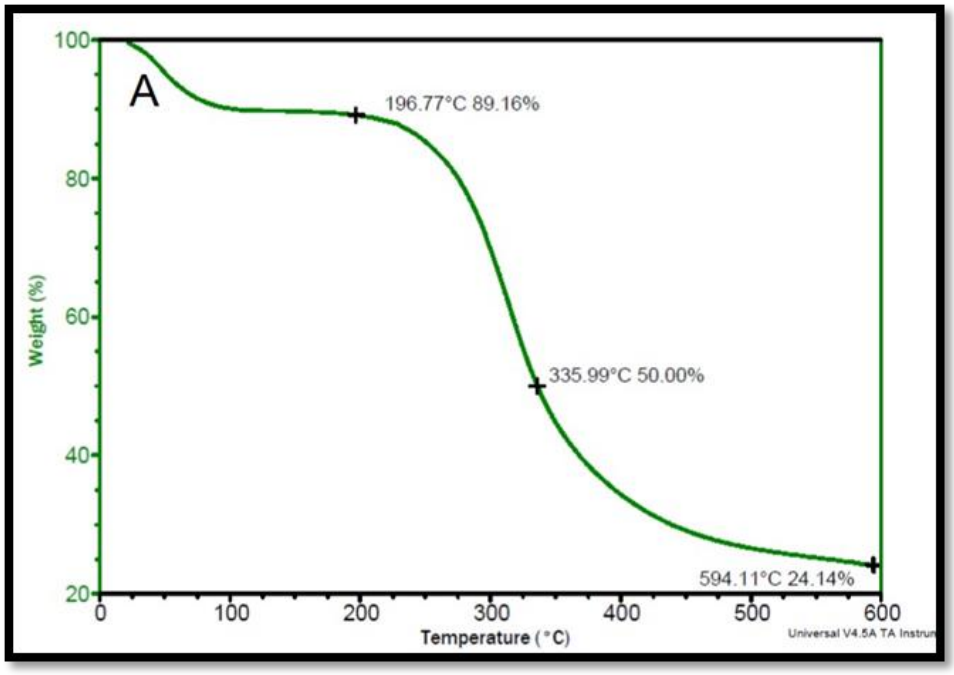

Fig.17A TGA Thermogram of C-ECM

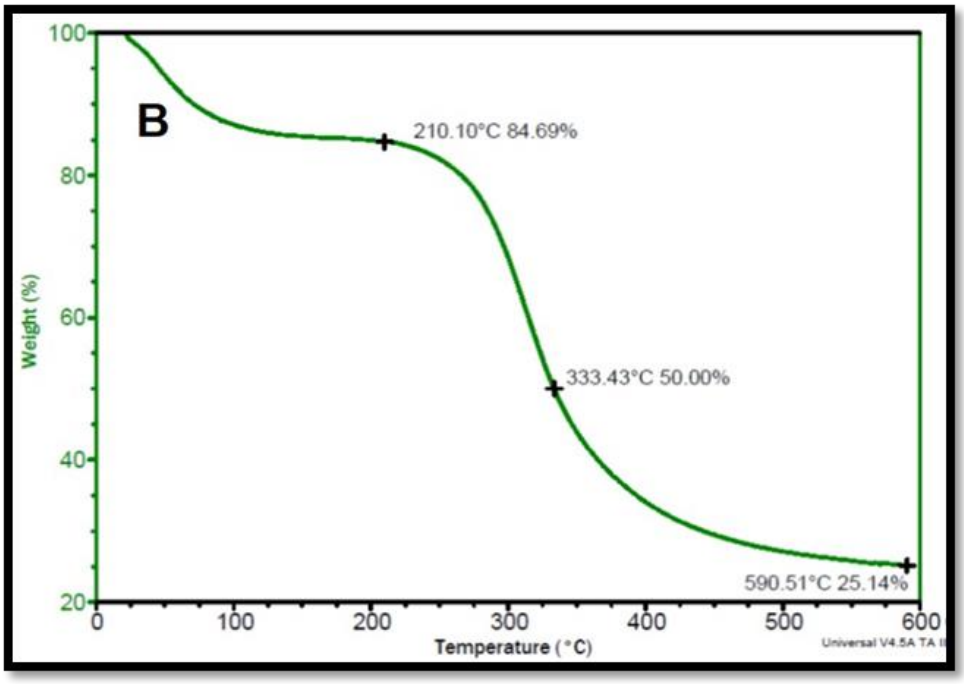

Fig.17B TGA Thermogram of Cys-AuNp CECM

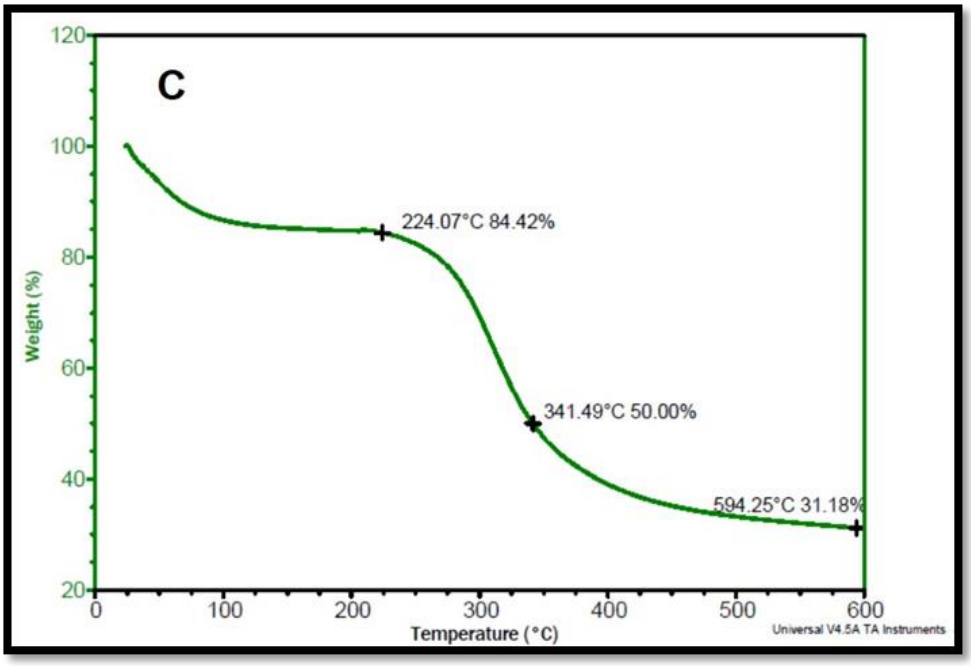

Fig 17C TGA Thermogram of GSH AuNp-CECM

Weight loss was observed mainly in three temperature ranges 100-200°C, 200-400°C and 400-600°C. The transition from room temperature to 200°C was due to the evaporation of physisorbed water and weight loss from 200-400°C was due to the decomposition of collagen molecules present in the scaffold (Iafisco et al., 2012). Slight weight loss between 500-600°C was due to the combustion of residual organic compounds present in the scaffold. Cys AuNp-CECM (25.14%) and GSH AuNp-CECM (31.18%) were found to have more residual components compared to C-ECM (24.14%). This confirmed the conjugation of gold nanoparticles on C-ECM, since metal particles are decomposed at higher temperatures.

5.5 Evaluation of Nanoparticle Retention on Scaffolds

The retention of gold nanoparticle on scaffolds were analysed by immersing Cys AuNp-CECM and GSH AuNp-CECM in Phosphate Buffered Saline(PBS) for 7 days and at the end of each 12 hours, samples were collected and UV visible spectra was measured. No corresponding characteristic peak of gold nanoparticle was observed even at the end of 7^{th} day. This confirmed the strong conjugation of gold nanoparticle on to the scaffolds.

4.6 Conductivity of the scaffolds

The conductivity of C-ECM was 69.86± 0.085µS/mm, that of Cys AuNp C-ECM and GSH AuNp C-ECM was 82.79±0.125 µS/mm and 84.59±0.44 µS/mm respectively (Fig.18). The conductivity of Cys AuNp C-ECM and GSH AuNp C-ECM were found to be higher than that of C-ECM which can be infered due to the presence of gold nanoparticles incorporated on the scaffold. Healthy heart tissue results in an effective intracellular conductivity of 0.16 S/m (longitudinal) and 0.005 S/m (transverse) and an effective extracellular conductivity of 0.21 S/m(longitudinal) and 0.06 S/m(transverse) (Stinstra et al., 2005). Thus the nano-gold coating made the C-ECM suitable for cardiac tissue engineering applications.

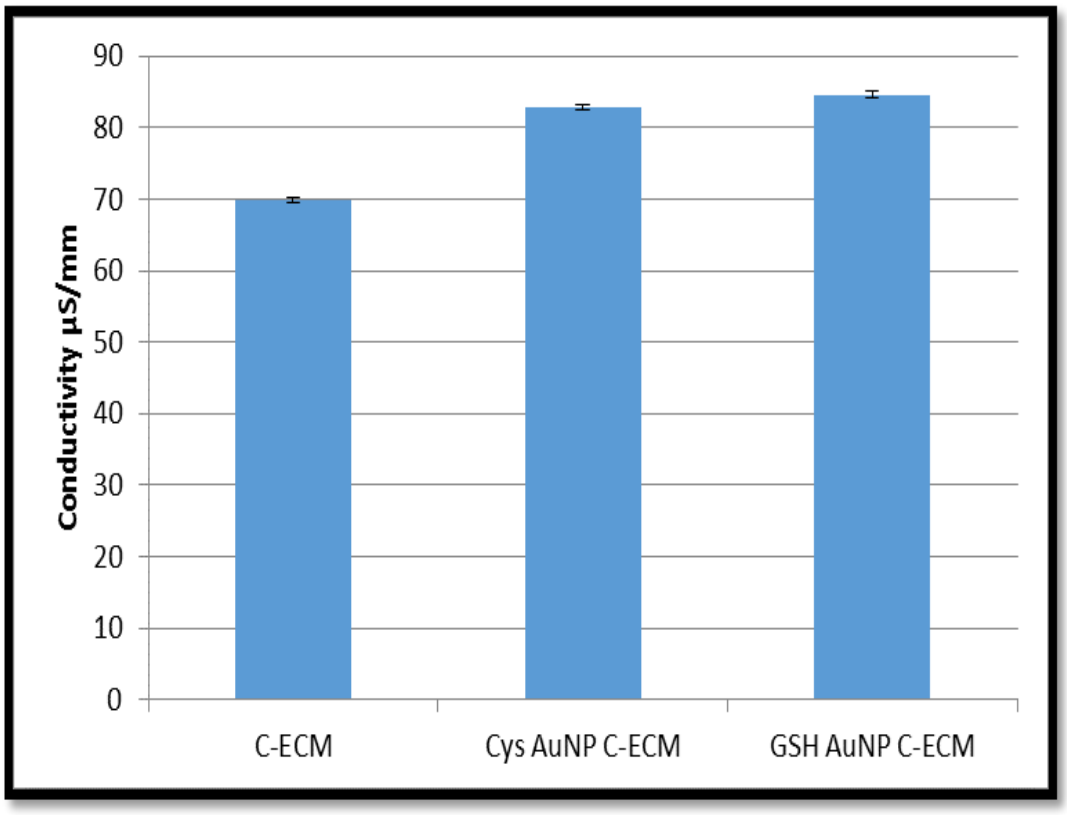

Fig. 18 Results of the conductivity studies performed on C-ECM, Cys -AuNp CECM and GSH-AuNp CECM

6. Biological Evaluation of Scaffolds

Biological evaluation of Cys AuNp-CECM and GSH AuNp-CECM were performed by cytotoxicity analysis and cell proliferation assay.

6.1 Cytotoxicity by Direct Contact Test

Direct contact test was performed to determine the cytotoxicity of C-CECM, Cys AuNp-CECM and GSH AuNp-CECM. Response of cells towards the scaffold were analysed when both came in contact. H9c2 cardiomyoblast monolayer showed non cytotoxicity for 24 hrs in direct contact with the scaffolds (Fig.19). Cell detachment, lysis and extensive vacuolization were absent when

they were in direct contact with each other. This was further confirmed by staining the cells with neutral red dye (Prasad et al., 2015)

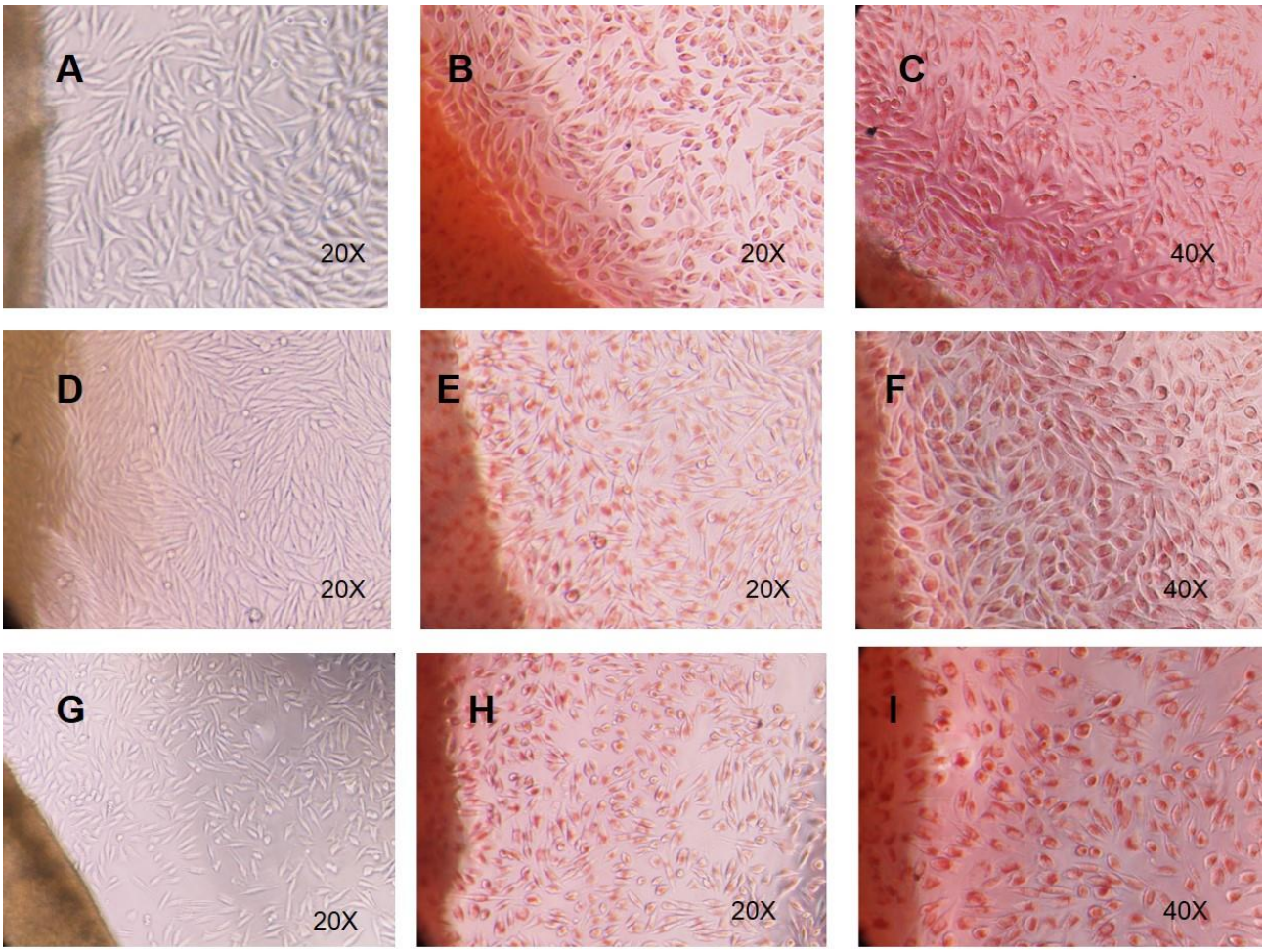

Fig 19. Phase contrast images of direct contact test and neutral staining showing non cytotoxicity of C-ECM(A-C) , Cys AuNp-CECM (D-F) and GSH AuNp-CECM (G-I)

6.2 Cytotoxicity by Test On Extract

Leachants from biomaterials may be toxic and was quantitatively evaluated by MTT assay of cells exposed to the leachants of the biomaterial. The scaffolds C-ECM, Cys AuNp-CECM and GSH AuNp-CECM were dipped in DMEM media for 24 hrs and the leachants were exposed to monolayer of H9c2 cells for the next 24 hrs and MTT assay was performed. Metabolic activity

of cells were calculated by taking cell control as 100%. H9c2 cells exposed to extracts of C-ECM, Cys AuNp-CECM and GSH AuNp-CECM showed 97.586±0.21%, 99.47±0.051% and 96.83±0.21% cell viability (Fig.20).The extracts from all the three scaffolds showed cell viability above 95%, so it can be concluded that there is cytocompatibility in using these scaffolds as a biomaterial (Prasad et al., 2015).

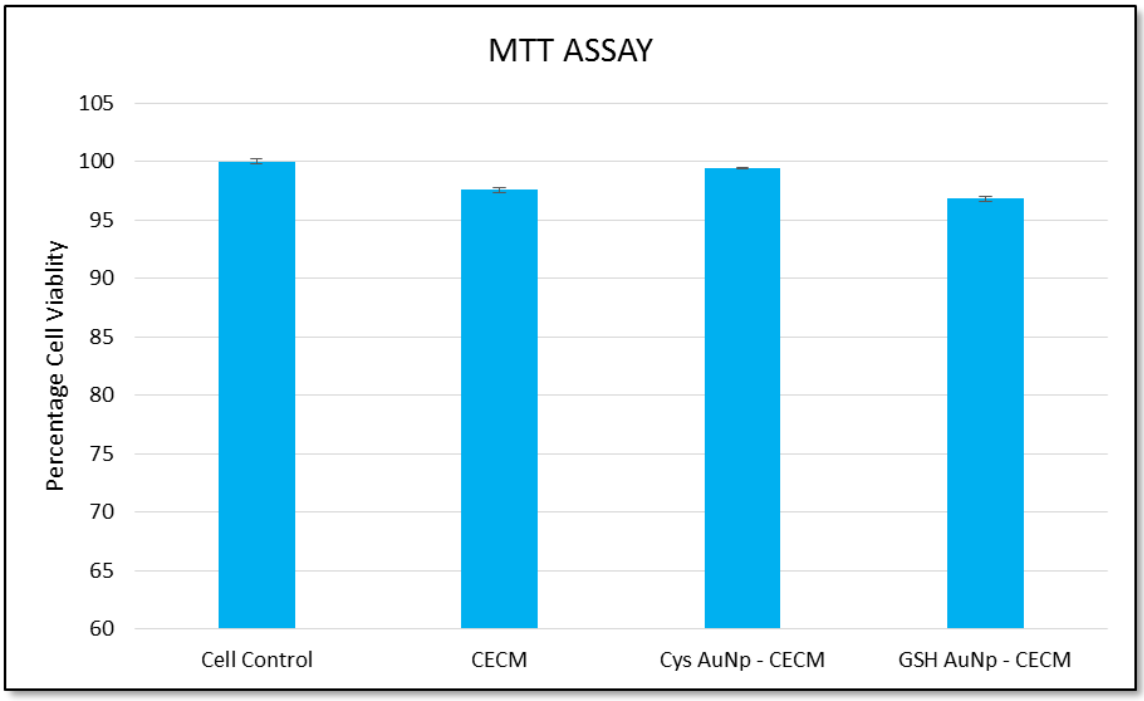

Fig 20. MTT assay of cells exposed to the extracts of C-ECM, Cys AuNp-CECM and GSH AuNp-CECM.

6.3 Live and Dead Staining

Viability of cells adhered on C-ECM, Cys- AuNp CECM and GSH-AuNp CECM were visualized by live and dead staining using FDA and PI (Prasad et al., 2015). The results showed that majority of the cells were viable (Fig.21). The cells were found both attached and invasive on these scaffolds. Live cells were prominent on Cys-AuNp CECM (Fig.22) scaffold.

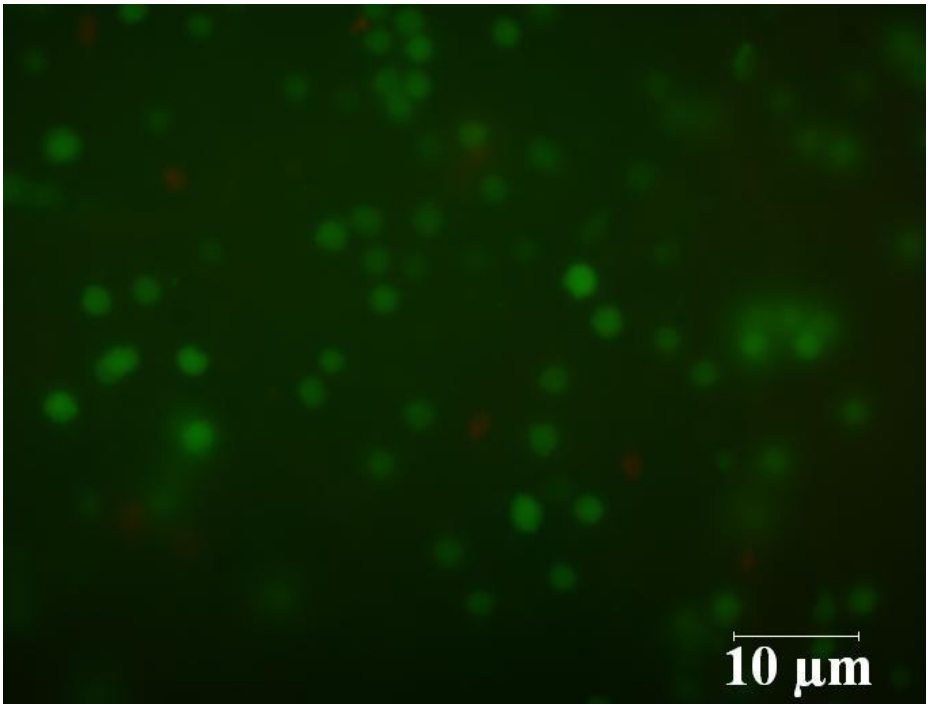

Fig.21 Fluorescent image of H9c2 cells seeded on C-ECM showing viable cells (green) and dead cells (red)

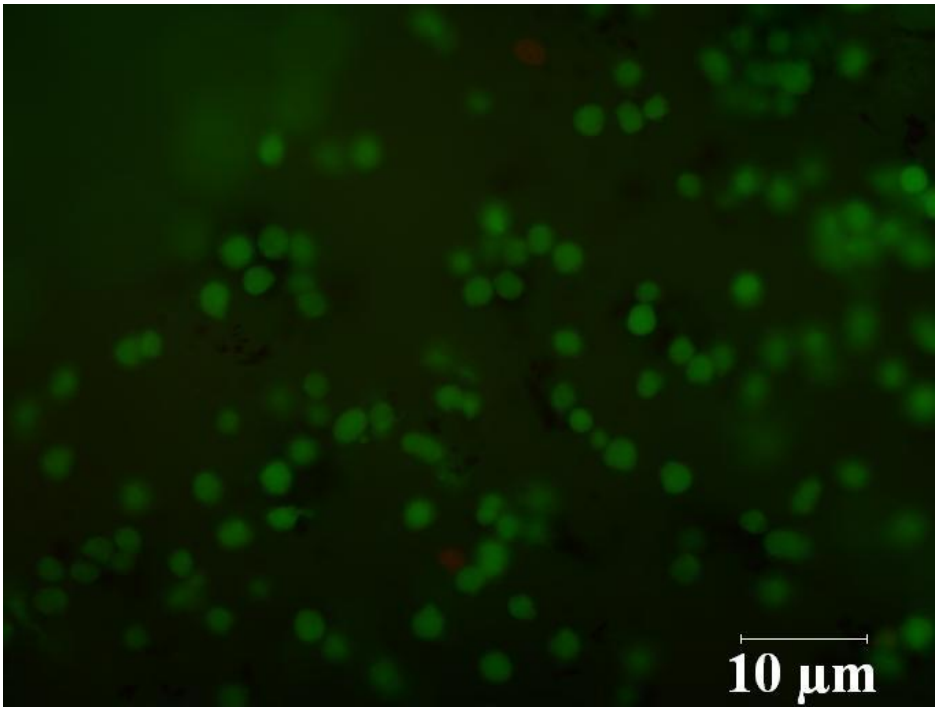

Fig.22 Fluorescent image of H9c2 cells seeded on Cys-AuNp CECM showing viable cells(green) and dead cells (red)

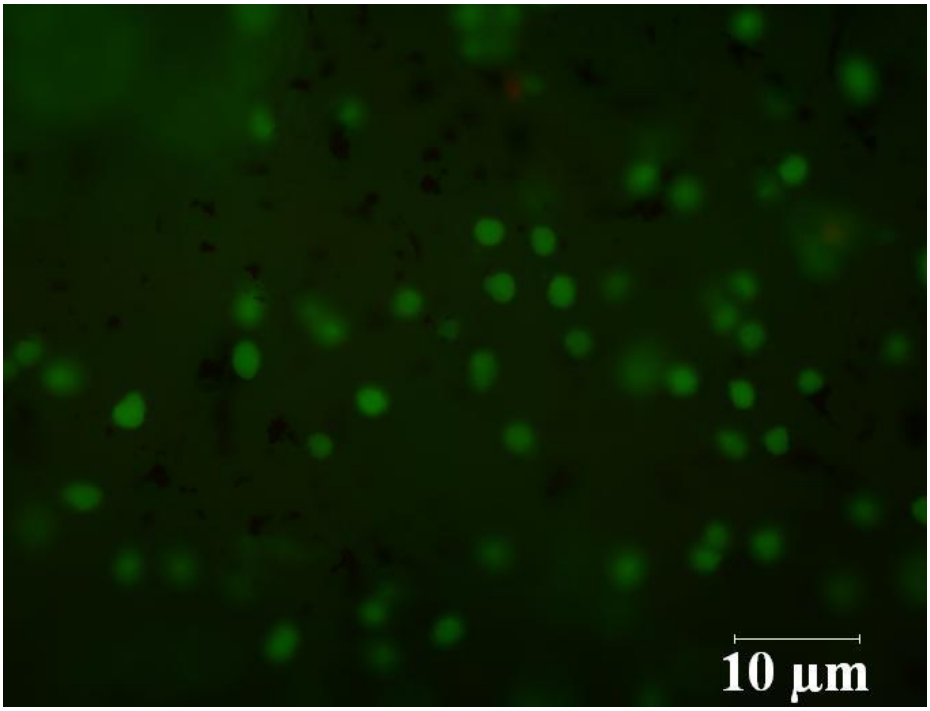

Fig.23 Fluorescent image of H9c2 cells seeded on GSH-AuNp CECM showing viable cells (green) and dead cells (red)

6.4 Cell proliferation Assay

H9c2 cells were seeded on C-ECM, Cys AuNp-CECM and GSH AuNp-CECM for 3 days and cell proliferation on these scaffolds were analysed by performing MTT assay (Prasad et al., 2015). Cell control were considered as 100% cell viability. Compared to C-ECM and GSH AuNp-CECM, cell proliferation was found more in Cys AuNp-CECM (Fig. 24) 87.08% cells were viable in the case of Cys AuNp-CECM. GSH AuNp-CECM showed 73.21% cell viability comparatively lower than C-ECM and Cys AuNp-CECM. Bare C–ECM (devoid of gold nanoparticle) showed 81.18% cell viability. There is less significant difference in viability of C-ECM as compared with Cys AuNp-CECM.

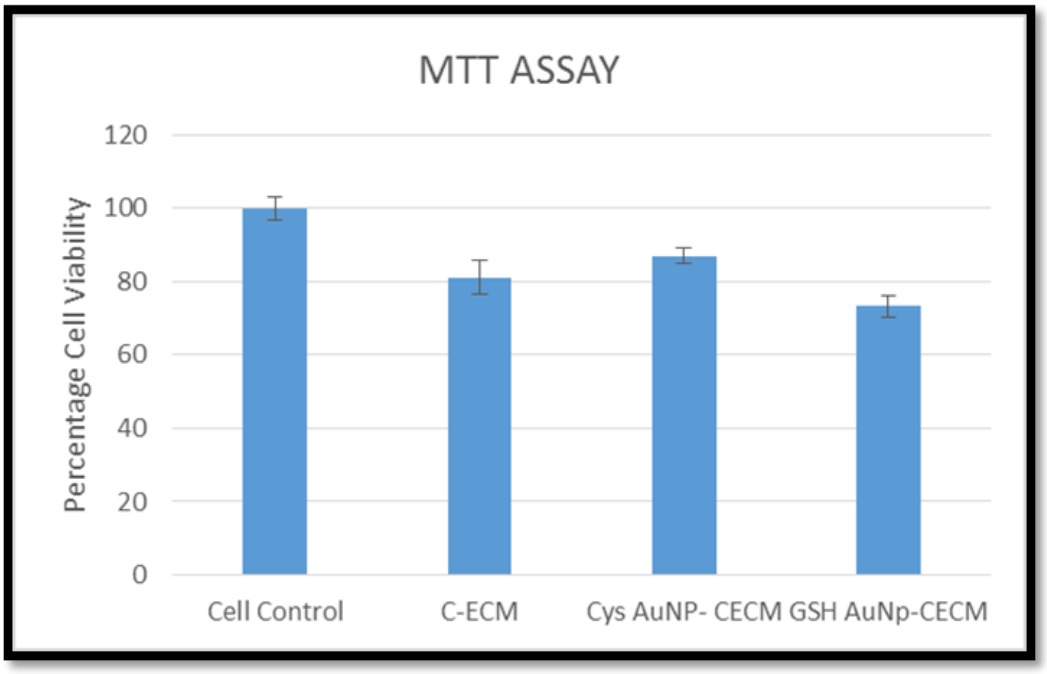

Fig. 24 Cell proliferation analysis of C-ECM, Cys AuNp-CECM and GSH AuNp by MTT assay

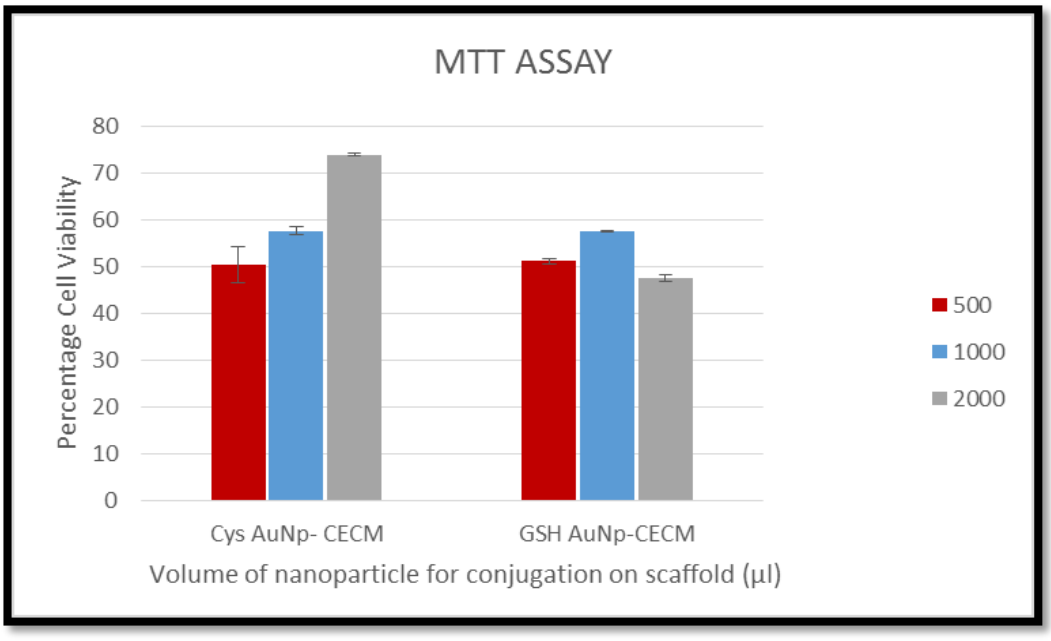

Fig.25 Comparative study on cell proliferation of Cys AuNp-CECM and GSH AuNp-CECM prepared by different concentrations.

Cell proliferation study was also performed on scaffolds prepared by different concentrations of Cys- AuNp for modifying C-ECM. Scaffolds were also prepared by different concentrations of GSH-AuNp and then the cell proliferation was studied by using MTT assay after 7 days. The modified C-ECM with the highest concentration of Cys -AuNp CECM appeared to have resulted in more cell proliferation compared with scaffolds modified by different concentrations of GSH-AuNp (Fig.25.)

SUMMARY AND CONCLUSION

Previous studies have shown that C-ECM have several potential tissue engineering applications like skin-graft for treating incision/burn wounds, buttressing staples for gastro-intestinal surgery and bladder augmentation. Against this background, this study explore the potential of C-ECM as a scaffold for cardiac tissue engineering. For achieving the objective, C-ECM was prepared by a non-detergent/enzymatic method and the gold nanoparticles of 15nm size were synthesized by citrate reduction method for conjugation. Characterization of gold nanoparticles were performed by UV visible spectroscopy, TEM and DLS .In order to couple the gold nanoparticles onto the scaffold, amine functionalization was performed with L-Cysteine or Glutathione by two methods; direct infiltration method and chemical crosslinking by EDC/NHS chemistry. The biomaterial properties of the synthesized gold nanoparticles were evaluated before and after amine functionalization. They were then incorporated on to C-ECM by activating the carboxyl groups by EDC and NHS reaction. The biomaterial properties of the gold nanoparticle conjugated C-ECM bionanocomposite resulting from the cysteine and glutathione functionalization were evaluated for its application in cardiac tissue engineering.

Successful incorporation of gold nanoparticle onto the scaffold was possible, as confirmed by results of EDS as well as thermogravimetric analysis, by chemical cross linking. However, the direct infiltration method for nanoparticle conjugation was deemed unsuccessful because the process did not retain the original micro-architecture of the scaffold. Further any other evidence for the gold nanoparticle incorporation was absent. Thermogravimetric analysis also indicated increased residual weight indicating the presence of metallic components in the bionanocomposite scaffold. From FTIR results it was confirmed that none of the processing steps of crosslinking resulted in denaturation of collagen structure of the ECM material. ESEM images

confirmed the fibrous architecture of the scaffold even after gold nanoparticle incorporation. Incorporation of gold nanoparticles enhanced the conductivity of scaffold compared to C-ECM. Further, the prototype was found to be cytocompatible and less cytotoxic to cardiomyoblast cells. This scaffold facilitated more cell proliferation and viability compared to that of pristine C-ECM and GSH-AuNp CECM. Remarkably, cells grown on Cys-AuNp CECM exhibited elongated and aligned morphological features expected for cardiomyoblast.

The gold nanoparticle conjugation did not affect the microarchitecture of the scaffold. Cysteine functionalization was preferred to glutathione functionalization for gold nanoparticle conjugation on C-ECM. The bionanocomposite of C-ECM prepared by conjugating cysteine functionalized gold nanoparticles had biomaterial properties of scaffolds used for cardiac tissue engineering.

In short, a candidate prototype of a bionanocomposite scaffold was prepared by incorporating gold nanoparticles onto porcine cholecyst derived extracellular matrix.

FUTURE PRESPECTIVES

Cysteine capped gold nanoparticle modified C-ECM may be useful for developing cardiac patch that could integrate and improve the heart function after conditions like myocardial infarction. This technique could also be useful for culturing other cells like neuronal cells that may assist to regenerate tissues such as injured spinal cord.

REFERENCES

- Aghajanloo, F., Nouroozi, S., Rostamizadeh, K., 2015. Safranin and cysteine capped gold nanoparticles: spectroscopic qualitative and quantitative studies. RSC Adv. 5, 11077–11083. doi:10.1039/C4RA15855E
- Anilkumar, T.V., Vineetha, V.P., Revi, D., Muhamed, J., Rajan, A., 2014. Biomaterial properties of cholecyst-derived scaffold recovered by a non-detergent/enzymatic method. J. Biomed. Mater. Res. B Appl. Biomater. 102, 1506–1516. doi:10.1002/jbm.b.33131
- Armour, A.D., Fish, J.S., Woodhouse, K.A., Semple, J.L., 2006. A comparison of human and porcine acellularized dermis: interactions with human fibroblasts in vitro. Plast. Reconstr. Surg. 117, 845–856. doi:10.1097/01.prs.0000204567.28952.9d
- Aryal, S., B K C, R., Dharmaraj, N., Bhattarai, N., Kim, C.H., Kim, H.Y., 2006. Spectroscopic identification of S-Au interaction in cysteine capped gold nanoparticles. Spectrochim. Acta. A. Mol. Biomol. Spectrosc. 63, 160–163. doi:10.1016/j.saa.2005.04.048
- Babensee, J.E., Anderson, J.M., McIntire, L.V., Mikos, A.G., 1998. Host response to tissue engineered devices. Adv. Drug Deliv. Rev., Tissue Engineering 33, 111–139. doi:10.1016/S0169-409X(98)00023-4
- Badylak, S.F., 2007. The extracellular matrix as a biologic scaffold material. Biomaterials 28, 3587–3593. doi:10.1016/j.biomaterials.2007.04.043
- Badylak, S.F., 2004. Xenogeneic extracellular matrix as a scaffold for tissue reconstruction. Transpl. Immunol. 12, 367–377. doi:10.1016/j.trim.2003.12.016
- Badylak, S.F., 2002. The extracellular matrix as a scaffold for tissue reconstruction. Semin. Cell Dev. Biol., Regeneration 13, 377–383. doi:10.1016/S1084952102000940
- Badylak, S.F., Gilbert, T.W., 2008. Immune Response to Biologic Scaffold Materials. Semin. Immunol. 20, 109–116. doi:10.1016/j.smim.2007.11.003
- Badylak, S.F., Lantz, G.C., Coffey, A., Geddes, L.A., 1989. Small intestinal submucosa as a large

diameter vascular graft in the dog. J. Surg. Res. 47, 74–80.

- Baranes, K., Shevach, M., Shefi, O., Dvir, T., 2016. Gold Nanoparticle-Decorated Scaffolds Promote Neuronal Differentiation and Maturation. Nano Lett. 16, 2916–2920. doi:10.1021/acs.nanolett.5b04033
- Bosman, F.T., Stamenkovic, I., 2003. Functional structure and composition of the extracellular matrix. J. Pathol. 200, 423–428. doi:10.1002/path.1437
- Brody, S., McMahon, J., Yao, L., O'Brien, M., Dockery, P., Pandit, A., 2007. The effect of cholecyst-derived extracellular matrix on the phenotypic behaviour of valvular endothelial and valvular interstitial cells. Biomaterials 28, 1461–1469. doi:10.1016/j.biomaterials.2006.11.030
- Brown, B., Lindberg, K., Reing, J., Stolz, D.B., Badylak, S.F., 2006. The basement membrane component of biologic scaffolds derived from extracellular matrix. Tissue Eng. 12, 519–526. doi:10.1089/ten.2006.12.519
- Brown, B.N., Badylak, S.F., 2014. Extracellular matrix as an inductive scaffold for functional tissue reconstruction. Transl. Res. J. Lab. Clin. Med. 163, 268–285. doi:10.1016/j.trsl.2013.11.003
- Burugapalli, K., Chan, J.C.Y., Kelly, J.L., Pandit, A., 2008. Buttressing staples with cholecyst-derived extracellular matrix (CEM) reinforces staple lines in an ex vivo peristaltic inflation model. Obes. Surg. 18, 1418–1423. doi:10.1007/s11695-008-9518-7
- Burugapalli, K., Chan, J.C.Y., Kelly, J.L., Pandit, A.S., 2014. Efficacy of Crosslinking on Tailoring In Vivo Biodegradability of Fibro-Porous Decellularized Extracellular Matrix and Restoration of Native Tissue Structure: A Quantitative Study using Stereology Methods. Macromol. Biosci. 14, 244–256. doi:10.1002/mabi.201300195
- Burugapalli, K., Chan, J.C.Y., Naik, H., Kelly, J.L., Pandit, A., 2009. Tailoring the properties of cholecyst-derived extracellular matrix using carbodiimide cross-linking. J. Biomater. Sci. Polym. Ed. 20, 1049–1063. doi:10.1163/156856209X444411

- Burugapalli, K., Pandit, A., 2007. Characterization of tissue response and in vivo degradation of cholecyst-derived extracellular matrix. Biomacromolecules 8, 3439–3451. doi:10.1021/bm700560k
- Burugapalli, K., Thapasimuttu, A., Chan, J.C.Y., Yao, L., Brody, S., Kelly, J.L., Pandit, A., 2007. Scaffold with a natural mesh-like architecture: isolation, structural, and in vitro characterization. Biomacromolecules 8, 928–936. doi:10.1021/bm061088x
- Castaneda, L., Valle, J., Yang, N., Pluskat, S., Slowinska, K., 2008. Collagen Crosslinking with Au Nanoparticles. Biomacromolecules 9, 3383–3388. doi:10.1021/bm800793z
- Cebotari, S., Lichtenberg, A., Tudorache, I., Hilfiker, A., Mertsching, H., Leyh, R., Breymann, T., Kallenbach, K., Maniuc, L., Batrinac, A., Repin, O., Maliga, O., Ciubotaru, A., Haverich, A., 2006. Clinical application of tissue engineered human heart valves using autologous progenitor cells. Circulation 114, I132–137. doi:10.1161/CIRCULATIONAHA.105.001065
- Chan, J.C.Y., Burugapalli, K., Naik, H., Kelly, J.L., Pandit, A., 2008. Amine functionalization of cholecyst-derived extracellular matrix with generation 1 PAMAM dendrimer. Biomacromolecules 9, 528–536. doi:10.1021/bm701055k
- Chen, F., Yoo, J.J., Atala, A., 1999. Acellular collagen matrix as a possible "off the shelf" biomaterial for urethral repair. Urology 54, 407–410.
- Chithrani, B.D., Ghazani, A.A., Chan, W.C.W., 2006. Determining the size and shape dependence of gold nanoparticle uptake into mammalian cells. Nano Lett. 6, 662–668. doi:10.1021/nl052396o
- Choi, H.R., Cho, K.A., Kang, H.T., Lee, J.B., Kaeberlein, M., Suh, Y., Chung, I.K., Park, S.C., 2011. Restoration of senescent human diploid fibroblasts by modulation of the extracellular matrix. Aging Cell 10, 148–157. doi:10.1111/j.1474-9726.2010.00654.x
- Coburn, J.C., Brody, S., Billiar, K.L., Pandit, A., 2007. Biaxial mechanical evaluation of cholecyst-derived extracellular matrix: a weakly anisotropic potential tissue engineered biomaterial. J. Biomed. Mater. Res. A 81, 250–256. doi:10.1002/jbm.a.30943

- Crapo, P.M., Gilbert, T.W., Badylak, S.F., 2011. An overview of tissue and whole organ decellularization processes. Biomaterials 32, 3233–3243. doi:10.1016/j.biomaterials.2011.01.057
- Dobrowolska, P., Krajewska, A., Gajda-Rączka, M., Bartosewicz, B., Nyga, P., Jankiewicz, B.J., 2015. Application of Turkevich Method for Gold Nanoparticles Synthesis to Fabrication of SiO2@Au and TiO2@Au Core-Shell Nanostructures. Materials 8, 2849–2862. doi:10.3390/ma8062849
- Domogatskaya, A., Rodin, S., Tryggvason, K., 2012. Functional diversity of laminins. Annu. Rev. Cell Dev. Biol. 28, 523–553. doi:10.1146/annurev-cellbio-101011-155750
- Duan, X., Sheardown, H., 2005. Crosslinking of collagen with dendrimers. J. Biomed. Mater. Res. A 75A, 510–518. doi:10.1002/jbm.a.30475
- Eckes, B., Nischt, R., Krieg, T., 2010. Cell-matrix interactions in dermal repair and scarring. Fibrogenesis Tissue Repair 3, 4. doi:10.1186/1755-1536-3-4
- Engler, A.J., Sen, S., Sweeney, H.L., Discher, D.E., 2006. Matrix elasticity directs stem cell lineage specification. Cell 126, 677–689. doi:10.1016/j.cell.2006.06.044
- Everts, M., Saini, V., Leddon, J.L., Kok, R.J., Stoff-Khalili, M., Preuss, M.A., Millican, C.L., Perkins, G., Brown, J.M., Bagaria, H., Nikles, D.E., Johnson, D.T., Zharov, V.P., Curiel, D.T., 2006. Covalently linked Au nanoparticles to a viral vector: potential for combined photothermal and gene cancer therapy. Nano Lett. 6, 587–591. doi:10.1021/nl0500555
- Fitzpatrick, J.C., Clark, P.M., Capaldi, F.M., Fitzpatrick, J.C., Clark, P.M., Capaldi, F.M., 2010. Effect of Decellularization Protocol on the Mechanical Behavior of Porcine Descending Aorta, Effect of Decellularization Protocol on the Mechanical Behavior of Porcine Descending Aorta. Int. J. Biomater. Int. J. Biomater. 2010, 2010, e620503. doi:10.1155/2010/620503, 10.1155/2010/620503
- Gao, J., Huang, X., Liu, H., Zan, F., Ren, J., 2012. Colloidal Stability of Gold Nanoparticles Modified with Thiol Compounds: Bioconjugation and Application in Cancer Cell Imaging.

Langmuir 28, 4464–4471. doi:10.1021/la204289k

- Gilbert, T.W., Sellaro, T.L., Badylak, S.F., 2006. Decellularization of tissues and organs. Biomaterials 27, 3675–3683. doi:10.1016/j.biomaterials.2006.02.014
- Gorschewsky, O., Puetz, A., Riechert, K., Klakow, A., Becker, R., 2005. Quantitative analysis of biochemical characteristics of bone-patellar tendon-bone allografts. Biomed. Mater. Eng. 15, 403–411.
- Heino, J., 2007. The collagen family members as cell adhesion proteins. BioEssays News Rev. Mol. Cell. Dev. Biol. 29, 1001–1010. doi:10.1002/bies.20636
- Hinterwirth, H., Wiedmer, S.K., Moilanen, M., Lehner, A., Allmaier, G., Waitz, T., Lindner, W., Lämmerhofer, M., 2013. Comparative method evaluation for size and size-distribution analysis of gold nanoparticles. J. Sep. Sci. 36, 2952–2961. doi:10.1002/jssc.201300460
- Hormozi-Nezhad, M.R., Seyedhosseini, E., Robatjazi, H., 2012a. Spectrophotometric determination of glutathione and cysteine based on aggregation of colloidal gold nanoparticles. Sci. Iran. 19, 958–963. doi:10.1016/j.scient.2012.04.018
- Hormozi-Nezhad, M.R., Seyedhosseini, E., Robatjazi, H., 2012b. Spectrophotometric determination of glutathione and cysteine based on aggregation of colloidal gold nanoparticles. Sci. Iran. 19, 958–963. doi:10.1016/j.scient.2012.04.018
- Houghton, A.M., Grisolano, J.L., Baumann, M.L., Kobayashi, D.K., Hautamaki, R.D., Nehring, L.C., Cornelius, L.A., Shapiro, S.D., 2006. Macrophage elastase (matrix metalloproteinase-12) suppresses growth of lung metastases. Cancer Res. 66, 6149–6155. doi:10.1158/0008-5472.CAN-04-0297
- Hutmacher, D.W., 2000. Scaffolds in tissue engineering bone and cartilage. Biomaterials, Orthopaedic Polymeric Biomaterials: Applications of Biodegradables 21, 2529–2543. doi:10.1016/S0142-9612(00)00121-6
- Hynes, R.O., 2009. Extracellular matrix: not just pretty fibrils. Science 326, 1216–1219.

doi:10.1126/science.1176009

- Iafisco, M., Foltran, I., Sabbatini, S., Tosi, G., Roveri, N., Iafisco, M., Foltran, I., Sabbatini, S., Tosi, G., Roveri, N., 2012. Electrospun Nanostructured Fibers of Collagen-Biomimetic Apatite on Titanium Alloy, Electrospun Nanostructured Fibers of Collagen-Biomimetic Apatite on Titanium Alloy. Bioinorg. Chem. Appl. Bioinorg. Chem. Appl. 2012, 2012, e123953. doi:10.1155/2012/123953, 10.1155/2012/123953
- Ikada, Y., 2006. Challenges in tissue engineering. J. R. Soc. Interface 3, 589–601. doi:10.1098/rsif.2006.0124
- Kajbafzadeh, A.-M., Sabetkish, S., Heidari, R., Ebadi, M., 2014. Tissue-engineered cholecyst-derived extracellular matrix: a biomaterial for in vivo autologous bladder muscular wall regeneration. Pediatr. Surg. Int. 30, 371–380. doi:10.1007/s00383-014-3474-1
- Kaszuba, M., Corbett, J., Watson, F.M., Jones, A., 2010. High-concentration zeta potential measurements using light-scattering techniques. Philos. Transact. A Math. Phys. Eng. Sci. 368, 4439–4451. doi:10.1098/rsta.2010.0175
- Kular, J.K., Basu, S., Sharma, R.I., 2014. The extracellular matrix: Structure, composition, age-related differences, tools for analysis and applications for tissue engineering. J. Tissue Eng. 5, 2041731414557112. doi:10.1177/2041731414557112
- Langer, R., 2000. Biomaterials in Drug Delivery and Tissue Engineering: One Laboratory's Experience. Acc. Chem. Res. 33, 94–101. doi:10.1021/ar9800993
- Larsen, M., Artym, V.V., Green, J.A., Yamada, K.M., 2006. The matrix reorganized: extracellular matrix remodeling and integrin signaling. Curr. Opin. Cell Biol. 18, 463–471. doi:10.1016/j.ceb.2006.08.009
- Lu, T., Li, Y., Chen, T., 2013. Techniques for fabrication and construction of three-dimensional scaffolds for tissue engineering. Int. J. Nanomedicine 8, 337–350. doi:10.2147/IJN.S38635
- Mao, X., Li, Z.-P., Tang, Z.-Y., 2010. One pot synthesis of monodispersed L-glutathione

stabilized gold nanoparticles for the detection of Pb2+ ions. Front. Mater. Sci. 5, 322–328. doi:10.1007/s11706-011-0118-4

- Miyagi, Y., Chiu, L.L.Y., Cimini, M., Weisel, R.D., Radisic, M., Li, R.-K., 2011. Biodegradable collagen patch with covalently immobilized VEGF for myocardial repair. Biomaterials 32, 1280–1290. doi:10.1016/j.biomaterials.2010.10.007
- Mohamed Anwar K Abdelhalim, M.M.M., 2012. Physical Properties of Different Gold Nanoparticles: Ultraviolet-Visibleand Fluorescence Measurements. Nanomedicine Amp Nanotechnol. 03. doi:10.4172/2157-7439.1000133
- Mondalek, F.G., Ashley, R.A., Roth, C.C., Kibar, Y., Shakir, N., Ihnat, M.A., Fung, K.-M., Grady, B.P., Kropp, B.P., Lin, H.-K., 2010. Enhanced angiogenesis of modified porcine small intestinal submucosa with hyaluronic acid-poly(lactide-co-glycolide) nanoparticles: from fabrication to preclinical validation. J. Biomed. Mater. Res. A 94, 712–719. doi:10.1002/jbm.a.32748
- Mondalek, F.G., Lawrence, B.J., Kropp, B.P., Grady, B.P., Fung, K.-M., Madihally, S.V., Lin, H.-K., 2008. The incorporation of poly(lactic-co-glycolic) acid nanoparticles into porcine small intestinal submucosa biomaterials. Biomaterials 29, 1159–1166. doi:10.1016/j.biomaterials.2007.11.020
- Mostow, E.N., Haraway, G.D., Dalsing, M., Hodde, J.P., King, D., OASIS Venus Ulcer Study Group, 2005. Effectiveness of an extracellular matrix graft (OASIS Wound Matrix) in the treatment of chronic leg ulcers: a randomized clinical trial. J. Vasc. Surg. 41, 837–843. doi:10.1016/j.jvs.2005.01.042
- Movasaghi, Z., Rehman, S., Rehman, D.I. ur, 2008. Fourier Transform Infrared (FTIR) Spectroscopy of Biological Tissues. Appl. Spectrosc. Rev. 43, 134–179. doi:10.1080/05704920701829043
- Muhamed, J., Rajan, A., Surendran, A., Jaleel, A., Anilkumar, T.V., 2015a. Comparative profiling of extractable proteins in extracellular matrices of porcine cholecyst and jejunum intended for

preparation of tissue engineering scaffolds. J. Biomed. Mater. Res. B Appl. Biomater. doi:10.1002/jbm.b.33567

- Muhamed, J., Revi, D., Rajan, A., Anilkumar, T.V., 2015b. Comparative local immunogenic potential of scaffolds prepared from porcine cholecyst, jejunum, and urinary bladder in rat subcutaneous model. J. Biomed. Mater. Res. B Appl. Biomater. 103, 1302–1311. doi:10.1002/jbm.b.33296
- Muhamed, J., Revi, D., Rajan, A., Geetha, S., Anilkumar, T.V., 2015c. Biocompatibility and Immunophenotypic Characterization of a Porcine Cholecyst-derived Scaffold Implanted in Rats. Toxicol. Pathol. 43, 536–545. doi:10.1177/0192623314550722
- Murry, C.E., Keller, G., 2008. Differentiation of embryonic stem cells to clinically relevant populations: lessons from embryonic development. Cell 132, 661–680. doi:10.1016/j.cell.2008.02.008
- Nezhad, Z.M., Poncelet, A., Kerchove, L. de, Gianello, P., Fervaille, C., Khoury, G.E., 2016. Small intestinal submucosa extracellular matrix (CorMatrix®) in cardiovascular surgery: a systematic review. Interact. Cardiovasc. Thorac. Surg. ivw020. doi:10.1093/icvts/ivw020
- O'Brien, F.J., 2011. Biomaterials & scaffolds for tissue engineering. Mater. Today 14, 88–95. doi:10.1016/S1369-7021(11)70058-X
- O'Reilly, M.S., Boehm, T., Shing, Y., Fukai, N., Vasios, G., Lane, W.S., Flynn, E., Birkhead, J.R., Olsen, B.R., Folkman, J., 1997. Endostatin: an endogenous inhibitor of angiogenesis and tumor growth. Cell 88, 277–285.
- Prasad, T., Shabeena, E.A., Vinod, D., Kumary, T.V., Anil Kumar, P.R., 2015. Characterization and in vitro evaluation of electrospun chitosan/polycaprolactone blend fibrous mat for skin tissue engineering. J. Mater. Sci. Mater. Med. 26, 5352. doi:10.1007/s10856-014-5352-8
- Ramchandran, R., Dhanabal, M., Volk, R., Waterman, M.J., Segal, M., Lu, H., Knebelmann, B., Sukhatme, V.P., 1999. Antiangiogenic activity of restin, NC10 domain of human collagen XV:

comparison to endostatin. Biochem. Biophys. Res. Commun. 255, 735–739. doi:10.1006/bbrc.1999.0248

- Rajeshwari, K.G., 2015. Interaction of Citrate-Capped Gold Nanoparticles with the Selected Amino Thiols for Sensing Applications. Proc. Natl. Acad. Sci. India - Sect. B Biol. Sci. doi:10.1007/s40011-015-0567-0

- Reing, J.E., Brown, B.N., Daly, K.A., Freund, J.M., Gilbert, T.W., Hsiong, S.X., Huber, A., Kullas, K.E., Tottey, S., Wolf, M.T., Badylak, S.F., 2010. The effects of processing methods upon mechanical and biologic properties of porcine dermal extracellular matrix scaffolds. Biomaterials 31, 8626–8633. doi:10.1016/j.biomaterials.2010.07.083
- Revi, D., Geetha, C., Thekkuveettil, A., Anilkumar, T.V., 2016. Fibroblast-loaded cholecyst-derived scaffold induces faster healing of full thickness burn wound in rabbit. J. Biomater. Appl. 30, 1036–1048. doi:10.1177/0885328215615759
- Revi, D., Vineetha, V.P., Muhamed, J., Rajan, A., Anilkumar, T.V., 2013. Porcine cholecyst–derived scaffold promotes full-thickness wound healing in rabbit. J. Tissue Eng. 4. doi:10.1177/2041731413518060
- Roth, C.C., Mondalek, F.G., Kibar, Y., Ashley, R.A., Bell, C.H., Califano, J.A., Madihally, S.V., Frimberger, D., Lin, H.-K., Kropp, B.P., 2011. Bladder regeneration in a canine model using hyaluronic acid-poly(lactic-co-glycolic-acid) nanoparticle modified porcine small intestinal submucosa. BJU Int. 108, 148–155. doi:10.1111/j.1464-410X.2010.09757.x
- Sarangi, S.N., Hussain, A.M.P., Sahu, S.N., 2009. Strong UV absorption and emission from L-cysteine capped monodispersed gold nanoparticles. Appl. Phys. Lett. 95, 073109. doi:10.1063/1.3210788
- Schuetz, T., Richmond, N., Harmon, M.E., Schuetz, J., Castaneda, L., Slowinska, K., 2013. The microstructure of collagen type I gel cross-linked with gold nanoparticles. Colloids Surf. B Biointerfaces 101, 118–125. doi:10.1016/j.colsurfb.2012.06.006

- Shahini, A., Yazdimamaghani, M., Walker, K.J., Eastman, M.A., Hatami-Marbini, H., Smith, B.J., Ricci, J.L., Madihally, S.V., Vashaee, D., Tayebi, L., 2013. 3D conductive nanocomposite scaffold for bone tissue engineering. Int. J. Nanomedicine 9, 167–181. doi:10.2147/IJN.S54668
- Shakya, P., Sharma, A.K., Kumar, N., Vellachi, R., Mathew, D.D., Dubey, P., Singh, K., Shrivastava, S., Shrivastava, S., Maiti, S.K., Hasan, A., Singh, K.P., 2016. Bubaline Cholecyst Derived Extracellular Matrix for Reconstruction of Full Thickness Skin Wounds in Rats. Scientifica 2016. doi:10.1155/2016/2638371
- Shevach, M., Fleischer, S., Shapira, A., Dvir, T., 2014. Gold Nanoparticle-Decellularized Matrix Hybrids for Cardiac Tissue Engineering. Nano Lett. 14, 5792–5796. doi:10.1021/nl502673m
- Shi, L., Ronfard, V., 2013. Biochemical and biomechanical characterization of porcine small intestinal submucosa (SIS): a mini review. Int. J. Burns Trauma 3, 173–179.
- Stinstra, J.G., Hopenfeld, B., Macleod, R.S., 2005. On the passive cardiac conductivity. Ann. Biomed. Eng. 33, 1743–1751. doi:10.1007/s10439-005-7257-7
- Streuli, C., 1999. Extracellular matrix remodelling and cellular differentiation. Curr. Opin. Cell Biol. 11, 634–640.
- Tanzer, M.L., 2006. Current concepts of extracellular matrix. J. Orthop. Sci. Off. J. Jpn. Orthop. Assoc. 11, 326–331. doi:10.1007/s00776-006-1012-2
- Turkevich, J., Stevenson, P.C., Hillier, J., 1951. A study of the nucleation and growth processes in the synthesis of colloidal gold. Discuss. Faraday Soc. 11, 55–75. doi:10.1039/DF9511100055
- Venugopal, J.R., Prabhakaran, M.P., Mukherjee, S., Ravichandran, R., Dan, K., Ramakrishna, S., 2012. Biomaterial strategies for alleviation of myocardial infarction. J. R. Soc. Interface R. Soc. 9, 1–19. doi:10.1098/rsif.2011.0301
- Walles, T., Herden, T., Haverich, A., Mertsching, H., 2003. Influence of scaffold thickness and scaffold composition on bioartificial graft survival. Biomaterials 24, 1233–1239.
- Wang, B., Borazjani, A., Tahai, M., Curry, A.L. de J., Simionescu, D.T., Guan, J., To, F., Elder,

S.H., Liao, J., 2010. Fabrication of cardiac patch with decellularized porcine myocardial scaffold and bone marrow mononuclear cells. J. Biomed. Mater. Res. A 94, 1100–1110. doi:10.1002/jbm.a.32781

- Wang, F., Liu, X., Lu, C.-H., Willner, I., 2013. Cysteine-Mediated Aggregation of Au Nanoparticles: The Development of a H2O2 Sensor and Oxidase-Based Biosensors. ACS Nano 7, 7278–7286. doi:10.1021/nn402810x
- Woods, T., Gratzer, P.F., 2005. Effectiveness of three extraction techniques in the development of a decellularized bone-anterior cruciate ligament-bone graft. Biomaterials 26, 7339–7349. doi:10.1016/j.biomaterials.2005.05.066
- Zheng, M.H., Chen, J., Kirilak, Y., Willers, C., Xu, J., Wood, D., 2005. Porcine small intestine submucosa (SIS) is not an acellular collagenous matrix and contains porcine DNA: possible implications in human implantation. J. Biomed. Mater. Res. B Appl. Biomater. 73, 61–67. doi:10.1002/jbm.b.30170